Plant Communications
Resource article

CellPress
Partner Journal

Enhancing wheat regeneration and genetic transformation through overexpression of *TaLAX1*

Yang Yu[1,2], Haixia Yu[1,2], Jing Peng[1], Wang Jinsong Yao[1], Yi Peng Wang[1], Feng Li Zhang[1], Shi Rong Wang[1], Yajie Zhao[1], Xiang Yu Zhao[1], Xian Sheng Zhang[1,*] and Ying Hua Su[1,*]

[1]State Key Laboratory of Crop Biology, College of Life Sciences, Shandong Agricultural University, Tai'an, Shandong 271018, China

[2]These authors contributed equally to this article.

***Correspondence: Ying Hua Su (suyh@sdau.edu.cn), Xian Sheng Zhang (zhangxs@sdau.edu.cn)**

https://doi.org/10.1016/j.xplc.2023.100738

ABSTRACT

In the realm of genetically transformed crops, the process of plant regeneration holds utmost significance. However, the low regeneration efficiency of several wheat varieties currently restricts the use of genetic transformation for gene functional analysis and improved crop production. This research explores overexpression of *TaLAX PANICLE1* (*TaLAX1*), which markedly enhances regeneration efficiency, thereby boosting genetic transformation and genome editing in wheat. Particularly noteworthy is the substantial increase in regeneration efficiency of common wheat varieties previously regarded as recalcitrant to genetic transformation. Our study shows that increased expression of *TaGROWTH-REGULATING FACTOR* (*TaGRF*) genes, alongside that of their co-factor, *TaGRF-INTERACTING FACTOR 1* (*TaGIF1*), enhances cytokinin accumulation and auxin response, which may play pivotal roles in the improved regeneration and transformation of *TaLAX1*-overexpressing wheat plants. Overexpression of *TaLAX1* homologs also significantly increases the regeneration efficiency of maize and soybean, suggesting that both monocot and dicot crops can benefit from this enhancement. Our findings shed light on a gene that enhances wheat genetic transformation and elucidate molecular mechanisms that potentially underlie wheat regeneration.

Key words: plant regeneration, genetic transformation, *TaLAX1*, TaGRF4–TaGIF1, cytokinin, auxin, wheat

Yu Y., Yu H., Peng J., Yao W.J., Wang Y.P., Zhang F.L., Wang S.R., Zhao Y., Zhao X.Y., Zhang X.S., and Su Y.H. (2024). Enhancing wheat regeneration and genetic transformation through overexpression of *TaLAX1*. Plant Comm. **5**, 100738.

INTRODUCTION

Recalcitrance to genetic transformation significantly limits the potential for transgenesis and genome editing in various plant species, including wheat, maize, barley, indica rice, and soybean (Shrawat and Lorz, 2006; Hiei et al., 2014). Reliable plant regeneration from transformed tissues is of paramount importance for efficient genetic transformation. However, the inefficiency of regeneration in many crops restricts transformation techniques such as *Agrobacterium*-mediated transformation and particle bombardment to a limited range of crop genotypes (Altpeter et al., 2016). Thus, regeneration represents a significant bottleneck to crop transformation. One recent advance in this field is the development of the PureWheat technique for *Agrobacterium*-mediated wheat transformation, which utilizes a modified tissue culture medium and an innovative transformant selection strategy (Ishida et al., 2015). Although PureWheat has demonstrated improvements in transformation efficiency for the model wheat genotype Fielder, it still remains ineffective for numerous commercial wheat cultivars (Wang et al., 2017). Consequently, there is a continued need for development of broadly applicable methods to enhance regeneration and transformation in wheat and other crop species.

Traditionally, *Agrobacterium*-mediated transformation and particle bombardment have been performed on immature embryos and other cultured tissues because of their efficient regeneration capabilities. Regeneration induction can be achieved by manipulating the expression of factors involved in somatic embryogenesis such as LEAFY COTYLEDON1 (LEC1), WUSCHEL (WUS), BABY BOOM (BBM), AGAMOUS-LIKE15 (AGL15), and SOMATIC EMBRYOGENESIS RECEPTOR KINASE (SERK) (Feher, 2015; Ikeuchi et al., 2016; Tang et al., 2020). These factors can reprogram somatic cells into totipotent cells, thereby enhancing regeneration efficiency in various plant genotypes (Lotan et al., 1998; Zuo et al., 2002a, 2002b; Boutilier et al., 2002; Bouchabke-Coussa et al., 2013; Florez et al., 2015; Lowe et al., 2016, 2018).

Published by the Plant Communications Shanghai Editorial Office in association with Cell Press, an imprint of Elsevier Inc., on behalf of CSPB and CEMPS, CAS.

Consequently, the regulated expression of such factors has been used to enhance crop transformation efficiency.

Overexpression of the maize *WUS2* and *BBM* genes has been shown to significantly enhance *Agrobacterium*-mediated transformation of previously non-transformable maize inbred lines. Similar improvements have also been observed in other recalcitrant crops such as rice, sorghum, and sugarcane (Lowe et al., 2016). However, overexpression of *BBM* and *WUS2* genes can lead to undesirable morphological abnormalities in transgenic maize plants, including thick and short roots, stunted and twisted phenotypes, and sterility. As a result, there is a demand for novel approaches or identification of new developmental regulators that can alleviate the pleiotropic effects associated with overexpression of these genes in regenerated plants.

Recently, a breakthrough approach that uses conditional expression drivers was reported to increase transformation efficiency without causing detrimental effects. Specifically, implementation of the maize phospholipid transferase protein promoter to drive expression of the *BBM* gene, in conjunction with an auxin-inducible *WUS2* gene, resulted in efficient transformation without any phenotypic abnormalities or sterility (Lowe et al., 2018; Gao et al., 2020). Furthermore, by linking the phospholipid transferase protein promoter with three viral enhancer elements, the expression of *WUS2* was amplified in somatic cells. This innovative system facilitates somatic embryogenesis without integration of *WUS2* upon infection with a mixture of *Agrobacterium* strains. Termed ‘‘altruistic transformation,’’ this method generates transgenic tissues capable of plant regeneration without the need for *WUS2* integration (Hoerster et al., 2020).

Expression of a fusion protein that combines wheat GROWTH-REGULATING FACTOR 4 (GRF4) and its co-factor GRF-INTERACTING FACTOR 1 (GIF1) has been used to enhance regeneration efficiency in non-transformable wheat genotypes (Debernardi et al., 2020; Qiu et al., 2022). In addition, overexpression of wheat *TaWOX5* has been found to significantly increase transformation efficiency not only in wheat but also in five other cereal species (Wang et al., 2022a).

Axillary meristems (AMs) play a crucial role in establishing plant architecture (McSteen and Leyser, 2005; Schmitz and Theres, 2005), and formation of AMs appears to be regulated by a conserved mechanism across different plant species (Woods et al., 2011). The rice *OsLAX PANICLE1* (*OsLAX1*) gene and the maize *ZmBARREN STALK1* (*ZmBA1*) gene encode non-canonical basic helix–loop–helix transcription factors that are orthologous to each other (Komatsu et al., 2003; Gallavotti et al., 2004). *OsLAX1* is essential for AM formation in rice, and mutants of *ZmBA1* in maize have unbranched and shortened tassels (Gallavotti et al., 2004). Similarly, mutations in the *Arabidopsis* ortholog *AtREGULATOR OF AXILLARY MERISTEM FORMATION* (*AtROX*) lead to impaired axillary bud formation during vegetative shoot development (Yang et al., 2012). However, it remains unclear whether a wheat ortholog of these genes is linked to AM formation. Although the protein sequence of wheat TaLAX1 is homologous to those of OsLAX1 and ZmBA1, its function differs from that of these orthologs. Mutants in *Talax1-aabbdd* exhibit a compact spike phenotype associated with the regulation of wheat domestication traits (He et al., 2021).

In this study, we present findings on the role of the TaLAX1 transcription factor in enhancing regeneration efficiency, genetic transformation, and genome editing in wheat. We demonstrate that overexpression of *TaLAX1-A* leads to upregulation of wheat *TaGRFs*, their co-factor *TaGIF1*, and cytokinin-biosynthesis and auxin-response genes. In addition, we provide evidence that *TaLAX1* homologs can stimulate regeneration in maize and soybean, suggesting the potential applicability of this approach to both monocot and dicot crops.

RESULTS

TaLAX1 overexpression enhances regeneration efficiency in the wheat genotype Fielder

In previous studies, OsLAX1 and ZmBA1, two non-canonical basic helix–loop–helix transcription factors, have been identified as crucial regulators of AM formation during vegetative and inflorescence development in rice and maize, respectively. These findings suggest that homologs of these genes in different plant species may share similar functions (Komatsu et al., 2003; Gallavotti et al., 2004). To identify wheat homologs of OsLAX1, denoted TaLAX1s, and investigate their role in wheat AM formation, we performed sequence analysis and examined the effects of overexpression. Through a BLAST search, we identified three homologous TaLAX1 proteins (TaLAX1-A, TaLAX1-B, and TaLAX1-D; Supplemental Figure 1A and 1B) in the common wheat line Chinese Spring (*Triticum aestivum*, AABBDD, $2n = 42$). These proteins exhibited significant amino acid identity with OsLAX1 (TaLAX1-A, 51.74%; TaLAX1-B, 53.91%; and TaLAX1-D, 52.81%).

To investigate the expression pattern of *TaLAX1*, we performed RNA *in situ* hybridization of wheat spike tissue sections (Supplemental Figure 1C–1F). *TaLAX1* transcripts initially accumulated in the spikelet meristem initiation sites (Supplemental Figure 1C) and later became restricted to a boundary region within the spikelet meristems (Supplemental Figure 1D and 1E). No *TaLAX1* mRNA was detected in floret tissues (Supplemental Figure 1F). These results suggest that *TaLAX1* may play a role in regulating meristematic cell proliferation, which is crucial for the development of spikelet meristems in the wheat spike.

To elucidate the function of *TaLAX1* in wheat, we created *myc*-tagged genomic constructs of *TaLAX1-A*, *TaLAX1-B*, and *TaLAX1-D* and inserted them into the PC186 expression vector (Hao et al., 2018) under the control of the maize *ZmUbi* promoter and *Nos* terminator. These constructs (PC186-*TaLAX1-myc*; Figure 1A) were introduced into the wheat genotype Fielder using the PureWheat *Agrobacterium*-mediated transformation method (Ishida et al., 2015). Interestingly, we observed a significant enhancement of shoot regeneration throughout the transformation process upon overexpression of *TaLAX1* (Figure 1B), consistent with its proposed role in initiation of meristematic cells. We calculated regeneration frequency as the number of calli that showed at least one regenerating shoot relative to the total number of inoculated embryos (Figure 1C). Regenerating shoot frequency was

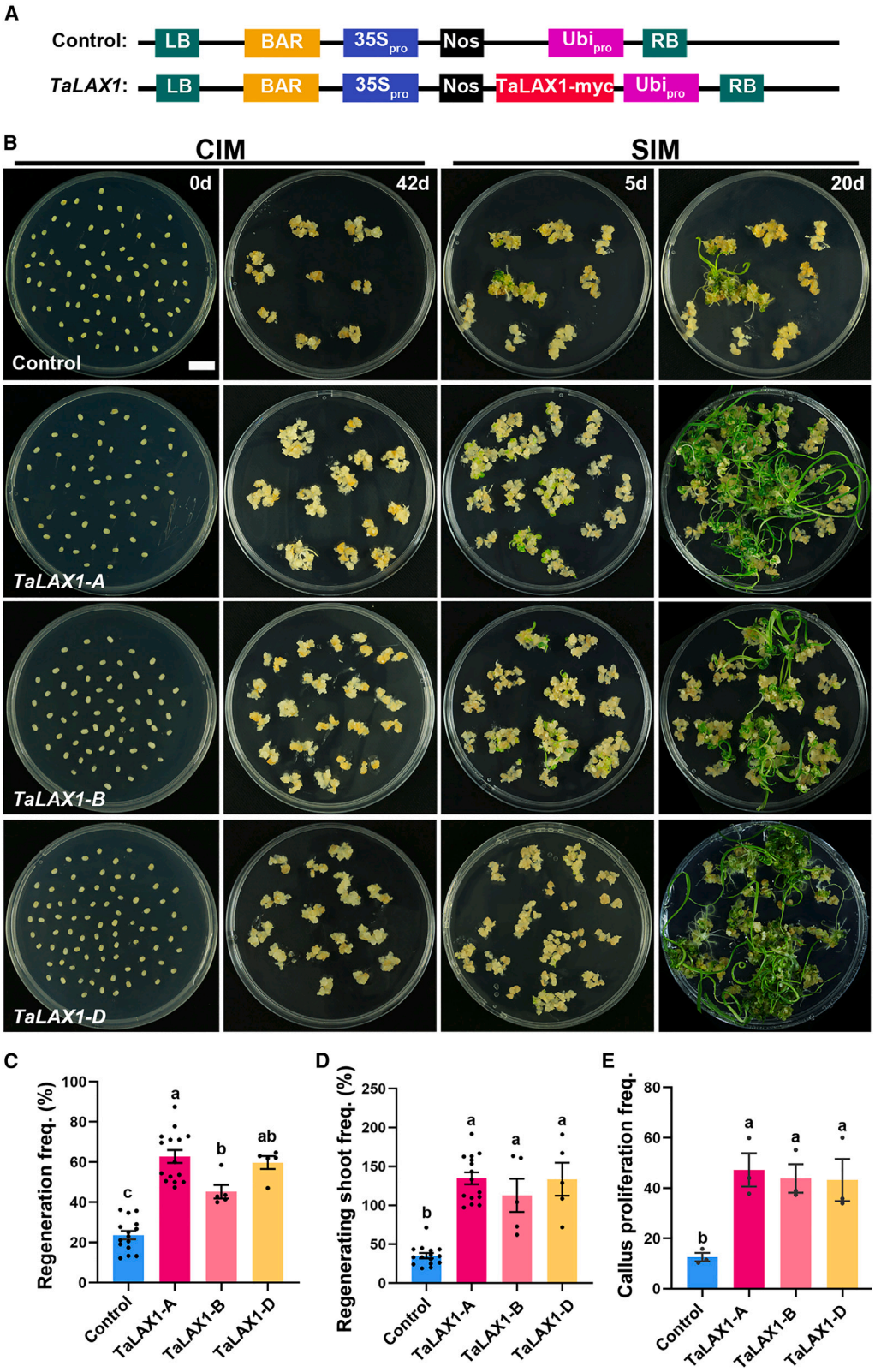

Figure 1. *TaLAX1* promotes shoot regeneration in the common wheat variety Fielder.

(A) Schematic representation of the PC186-*TaLAX1-myc* vector with the *ZmUbi* promoter and *Nos* terminator; the PC186 empty vector was used as a control.

(B) Shoot regeneration phenotypes of immature embryos infected with the empty vector (control) or PC186-*TaLAX1-A/B/D-myc* vector. CIM, callus induction medium (including WLS-AS, WLS-Res, WLS-P5, and WLS-P10 media in the PureWheat transformation); SIM, shoot induction medium (LSZ-P5

(legend continued on next page)

calculated as the number of regenerating shoots per total number of inoculated embryos (Figure 1D). The average regeneration frequency was significantly higher in *TaLAX1* transgenic calli (*TaLAX1-A*, 62.76% ± 3.24%; *TaLAX1-B*, 45.26% ± 3.37%; *TaLAX1-D*, 59.77% ± 3.22%) than in calli with the PC186 empty vector control (23.65% ± 2.08%; Figure 1C and Supplemental Data 1). Similarly, the regenerating shoot frequency was significantly higher in *TaLAX1 transgenic calli* than in the control (*TaLAX1-A*, 134.63% ± 7.75%; *TaLAX1-B*, 112.73% ± 21.33%; *TaLAX1-D*, 133.51% ± 21.10% vs. empty vector control, 35.20% ± 3.39%) (Figure 1D and Supplemental Data 1). Moreover, *TaLAX1* overexpression also accelerated callus proliferation, as indicated by the greater increase in weight of transgenic calli after induction (Figure 1E and Supplemental Data 2). Among the *TaLAX1* homologs, *TaLAX1-A* exhibited the highest regeneration frequency (Figure 1C) and transcript levels at each stage of regeneration (Supplemental Figure 2), leading us to focus on *TaLAX1-A* for further analysis.

TaLAX1-A promotes shoot regeneration in different wheat genotypes

To explore the potential impact of *TaLAX1* on shoot regeneration, we introduced the PC186-*TaLAX1-A-myc* (*TaLAX1-A*-OE) vector into five common wheat varieties (Chinese Spring, Kenong 199, Shannong 28, Aikang 58, and Jimai 22) and two durum wheat varieties (Langdon and Kronos), including varieties known to be recalcitrant to transformation (Figure 2A). We observed a significant enhancement of regeneration frequency, regenerating shoot frequency, and callus proliferation frequency in *TaLAX1-A*-OE transgenic calli across all varieties compared with the empty vector control (Figure 2B–2D and Supplemental Data 3 and 4). Notably, Aikang 58 and Jimai 22, which are widely cultivated in China, with a planting area exceeding 2 million hectares each, displayed poor callus quality and were recalcitrant to regeneration in the control groups. However, overexpression of *TaLAX1-A* dramatically improved callus proliferation in both Aikang 58 and Jimai 22 (Figure 2B and Supplemental Data 3). The regeneration frequency significantly increased from 3.83% ± 1.82% to 31.34% ± 3.67% in Aikang 58 and from 2.22% ± 1.48% to 35.62% ± 10.76% in Jimai 22 in response to *TaLAX1-A* overexpression (Figure 2C and Supplemental Data 4). In addition, there was a notable increase in the number of regenerating shoots per immature embryo in these varieties (Figure 2D and Supplemental Data 4).

For the T1 progeny of transgenic lines overexpressing *TaLAX1-A* in Fielder and Chinese Spring, genotyping analyses confirmed the presence of the transgene, and the plants were found to be fertile, with increased effective tiller numbers in both varieties (Supplemental Figure 3 and Supplemental Data 5). Consistent with previous findings, overexpression of *TaLAX1-A* resulted in significant increases in spike length and plant height, which resembled the phenotypes observed in transgenic lines overexpressing *TaLAX1-D* (He et al., 2021). We measured the regeneration frequencies and regenerating shoot frequencies of embryos from T1 transgenic lines and found significant increases in both frequencies compared with the control non-transgenic lines (Figure 3A–3C and 3E–3G and Supplemental Data 6). To investigate the specific effect of reduced *TaLAX1-A* expression on wheat regeneration while keeping *TaLAX1-B/D* expression levels unchanged, we selected the *TaLAX1-A* promoter region, which has relatively low similarity to the *TaLAX1-B/TaLAX1-D* promoter sequences (*TaLAX1-Apro* vs. *TaLAX1-Bpro*, 48.38%; *TaLAX1-Apro* vs. *TaLAX1-Dpro*, 70.98%), rather than the highly similar gene regions (*TaLAX1-A* vs. *TaLAX1-B*, 88.78%; *TaLAX1-A* vs. *TaLAX1-D*, 93.63%), as the target for CRISPR–Cas9. We obtained two independent lines (*talax1-a-cr* 1# and 2#) with deletions in the *TaLAX1-A* promoter that resulted in reduced *TaLAX1-A* expression compared with wild-type Fielder; the expression levels of *TaLAX1-B* and *TaLAX1-D* showed no significant changes (Figure 3I and 3J). Significantly lower regeneration frequency was observed in the T1 progeny of the *talax1-a-cr* lines compared with wild-type Fielder (Figure 3K and Supplemental Data 7). These findings demonstrate the heritability of *TaLAX1-A* function in improving shoot regeneration.

To further test the broad-spectrum regenerative effects of *TaLAX1-A*, we introduced *TaLAX1-A*-OE and empty control vectors into wild-type Fielder using traditional particle bombardment-mediated transformation. The plants transformed with *TaLAX1-A* showed higher regeneration frequencies (37.83% ± 1.46%) than the controls (17.58% ± 2.42%; Supplemental Figure 4A–4C and Supplemental Data 8). Similarly, the regenerating shoot frequency was significantly higher in plants transformed with *TaLAX1-A* than in controls (Supplemental Figure 4D and Supplemental Data 8). Collectively, these results demonstrate the ability of *TaLAX1-A* overexpression to improve wheat regeneration in different varieties and with different protocols.

TaLAX1-A improves transformation and gene editing efficiency in wheat

Efficient regeneration is crucial for successful plant genetic transformation. To assess the effect of *TaLAX1-A* on the transformation frequency of wheat, we generated a compound expression vector (*TaLAX1-A*-OE-*GUS*) by combining Ubi_{pro}:*TaLAX1* with Ubi_{pro}:*GUS* cassettes. Transformation experiments were performed in the common wheat variety Fielder, and the regeneration and transformation frequencies were estimated. The wheat *TaLAX1-A*-OE-*GUS* transgene significantly increased regeneration frequency

in the PureWheat transformation); 0d and 42d, immature embryos were placed on CIM for 0 or 42 days; 5d and 20d, immature embryos were placed on CIM for 42 days and then transferred to SIM for 5 days or 20 days. Scale bar, 1 cm.

(C) Regeneration frequencies of immature embryos infected with control or PC186-*TaLAX1-A/B/D-myc* vector. Regeneration frequency = no. of calli showing at least one regenerating shoot/no. of inoculated embryos × 100%.

(D) Regenerating shoot frequencies of immature embryos infected with control or PC186-*TaLAX1-A/B/D-myc* vector. Regenerating shoot frequency = no. of regenerating shoots/no. of inoculated embryos × 100%.

(E) Callus proliferation frequencies of immature embryos infected with control or PC186-*TaLAX1-A/B/D-myc* vector. Callus proliferation frequency = increased weight of callus after induction on CIM for 42 days/weight of immature embryos before induction. Values in **(C–E)** are means ± SEM from at least three independent experiments. Black points are the results from individual experiments. One-way ANOVA and Tukey's multiple comparison tests were performed. Different lowercase letters indicate statistically significant differences ($P < 0.05$).

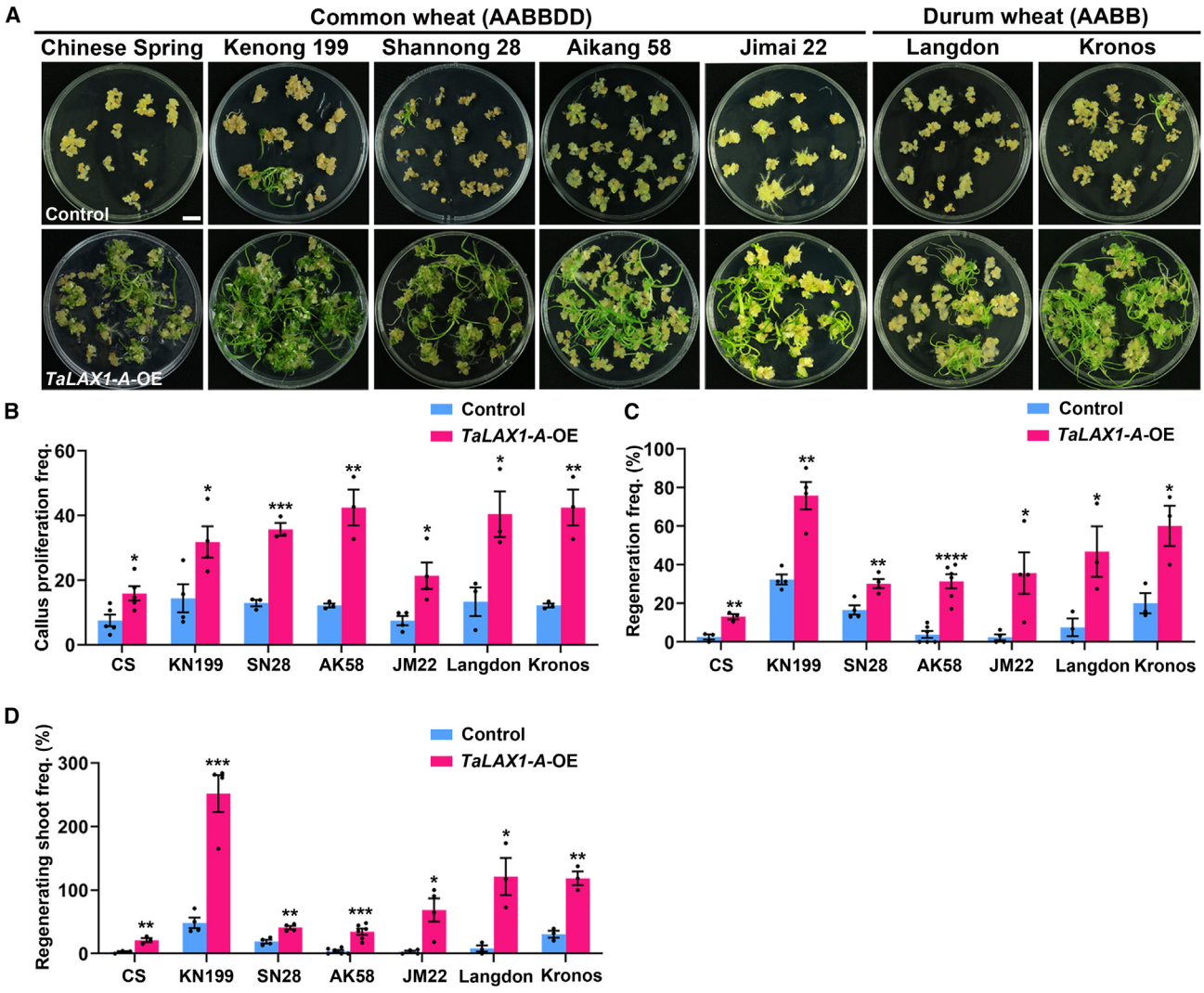

Figure 2. Overexpression of *TaLAX1-A* promotes shoot regeneration in different wheat genotypes.

(A) Shoot regeneration phenotypes of immature wheat embryos of different genotypes infected with empty vector (control) or *TaLAX1-A*-OE vector. Scale bar, 1 cm.

(B) Callus proliferation frequencies of wheat immature embryos of different genotypes infected with control or *TaLAX1-A*-OE vector.

(C) Regeneration frequencies of wheat immature embryos of different genotypes infected with control or *TaLAX1-A*-OE vector.

(D) Regenerating shoot frequencies of wheat immature embryos of different genotypes infected with control or *TaLAX1-A*-OE vector. CS, Chinese Spring; KN199, Kenong 199; SN28, Shannong 28; AK58, Aikang 58; JM22, Jimai 22. Values in **(B–D)** are means ± SEM from at least three independent experiments. Black points are the results from individual experiments. ****$P < 0.0001$; ***$P < 0.001$; **$P < 0.01$; *$P < 0.05$ (Student's *t*-test, two-tailed).

compared with the control (Ubi_{pro}*:GUS* alone; Figure 4A and 4B and Supplemental Data 9). Consistent with this finding, the transformation frequency with the *TaLAX1-A*-OE-*GUS* expression cassette (79.52% ± 5.43%) was significantly higher than that of the control (38.46% ± 6.17%; Figure 4B and Supplemental Data 9). Improved regeneration and transformation frequencies were also observed when a mixture of *Agrobacterium* strains was used, one carrying the *TaLAX1-A*-OE expression cassette and the other carrying the Ubi_{pro}*:GUS* marker cassette (Supplemental Figure 5). Transgenic plants with *GUS* expression signals revealed higher efficiency in the *TaLAX1-A*-OE and *GUS* co-transformation experiments than in co-transformation experiments with the empty vector and *GUS* vector (Supplemental Figure 5 and Supplemental Data 10), suggesting that *TaLAX1-A* overexpression enhanced transformation frequency.

Next, the transformation frequencies of the *TaLAX1-A*-OE and *talax1-a-cr* lines were evaluated using the Ubi_{pro}*:GUS* vector. The *TaLAX1-A*-OE transgenic lines showed significantly higher transformation frequencies than the non-transgenic lines (Figure 3D and 3H and Supplemental Data 6), whereas the *talax1-a-cr* transgenic lines exhibited much lower transformation frequencies than wild-type Fielder (Figure 3L and Supplemental Data 7). These results indicate that *TaLAX1-A* overexpression not only enhances shoot regeneration but also improves transformation efficiency in wheat.

The effect of *TaLAX1-A*-improved transformation on CRISPR–Cas9-mediated genome editing frequency was also investigated and compared with conventional transformation. The *Q* gene, which encodes an AP2-like transcription factor, is essential in

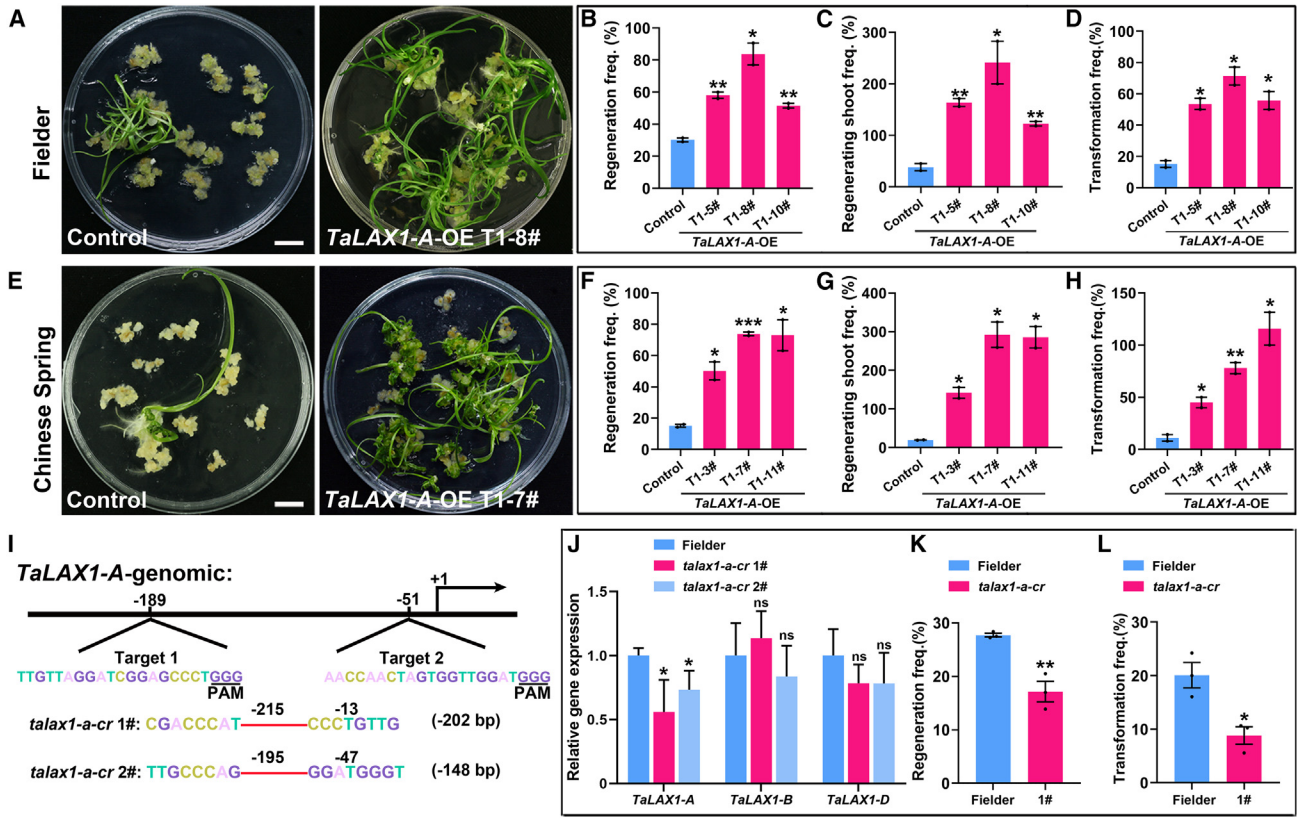

Figure 3. The function of *TaLAX1-A* in regeneration is heritable.

(A) Shoot regeneration phenotypes in Fielder T1 progeny of non-transgenic lines (control) or the *TaLAX1-A*-OE T1-8# transgenic line infected with the Ubi_{pro}*:GUS* vector. Scale bar, 1 cm.

(B) Regeneration frequencies of control and *TaLAX1-A*-OE T1-5#, *TaLAX1-A*-OE T1-8#, and *TaLAX1-A*-OE T1-10# lines in Fielder.

(C) Regenerating shoot frequencies of control and *TaLAX1-A*-OE T1-5#, *TaLAX1-A*-OE T1-8#, and *TaLAX1-A*-OE T1-10# lines in Fielder.

(D) Transformation frequencies of control and *TaLAX1-A*-OE T1-5#, *TaLAX1-A*-OE T1-8#, and *TaLAX1-A*-OE T1-10# lines in Fielder. Transformation frequency = no. of transgenic shoots with GUS signals/no. of inoculated embryos × 100%.

(E) Shoot regeneration phenotypes in Chinese Spring T1 progeny of non-transgenic lines (control) or the *TaLAX1-A*-OE T1-7# transgenic line infected with the Ubi_{pro}*:GUS* vector. Scale bar, 1 cm.

(F) Regeneration frequencies of control and *TaLAX1-A*-OE T1-3#, *TaLAX1-A*-OE T1-7#, and *TaLAX1-A*-OE T1-11# lines in Chinese Spring.

(G) Regenerating shoot frequencies of control and *TaLAX1-A*-OE T1-3#, *TaLAX1-A*-OE T1-7#, and *TaLAX1-A*-OE T1-11# lines in Chinese Spring.

(H) Transformation frequencies of control and *TaLAX1-A*-OE T1-3#, *TaLAX1-A*-OE T1-7#, and *TaLAX1-A*-OE T1-11# lines in Chinese Spring.

(I) Generation of *TaLAX1-A* knockdown lines by CRISPR–Cas9. Two target sites in the promoter of *TaLAX1-A* are shown. PAM, protospacer-adjacent motif.

(J) Relative expression of *TaLAX1-A/B/D* in the wild type and two *talax1-a-cr* transgenic lines of Fielder.

(K) Regeneration frequencies of the wild type and *talax1-a-cr* 1# transgenic line in Fielder.

(L) Transformation frequencies of the wild type and *talax1-a-cr* 1# transgenic line in Fielder. Values in **(B)–(D)**, **(F)–(H)**, **(K), and (L)** are means ± SEM; values in **(J)** are means ± SD. All experiments were performed at least two times. Black points are the results from individual experiments. ***$P < 0.001$; **$P < 0.01$; *$P < 0.05$; ns, not significant (Student's *t*-test, two-tailed).

wheat domestication and affects the number of florets in spikelets (Zhang et al., 2011). A binary vector containing a cassette with *TaLAX1-A*-OE, Cas9, and a guide RNA targeting the *Q* gene (Figure 4C) was generated for use in *Agrobacterium* transformation (*TaLAX1-A*-OE-*Q-CRISPR*). The *Q-CRISPR* construct served as the control. As expected, regeneration frequency was significantly higher in the *TaLAX1-A*-OE group than in the control (Figure 4D and 4E and Supplemental Data 11). The genome editing frequency, calculated as the number of T0 plants with an edited *Q* gene relative to the total number of inoculated embryos, was significantly higher in the *TaLAX1-A*-OE context (35.88% ± 6.90%) than in the control (11.19% ± 2.48%; Figure 4E and Supplemental Data 11). However, the proportion of *Q*-gene-edited T0 shoots in the total number of T0 plants did not differ significantly from that of the control (Figure 4E and Supplemental Data 11). This suggests that the enhanced editing frequencies resulting from *TaLAX1-A* can be attributed to improved rates of regeneration. In addition, successful Cas9-induced *Q*-gene editing was detected in 12 independent *TaLAX1-A*-OE-*q-cr* T0 lines, and 6 lines exhibited clear mutant *q*-null phenotypes (Figure 4F and 4G and Supplemental Data 11 and 12). Overall, *TaLAX1-A* overexpression significantly enhanced gene editing frequency. Because both the *Q-CRISPR* and the *TaLAX1-A*-OE sequences can be segregated out after editing the desired genomic region, the *TaLAX1* strategy is ideal for extending genome editing technology to wheat varieties with low regeneration efficiency.

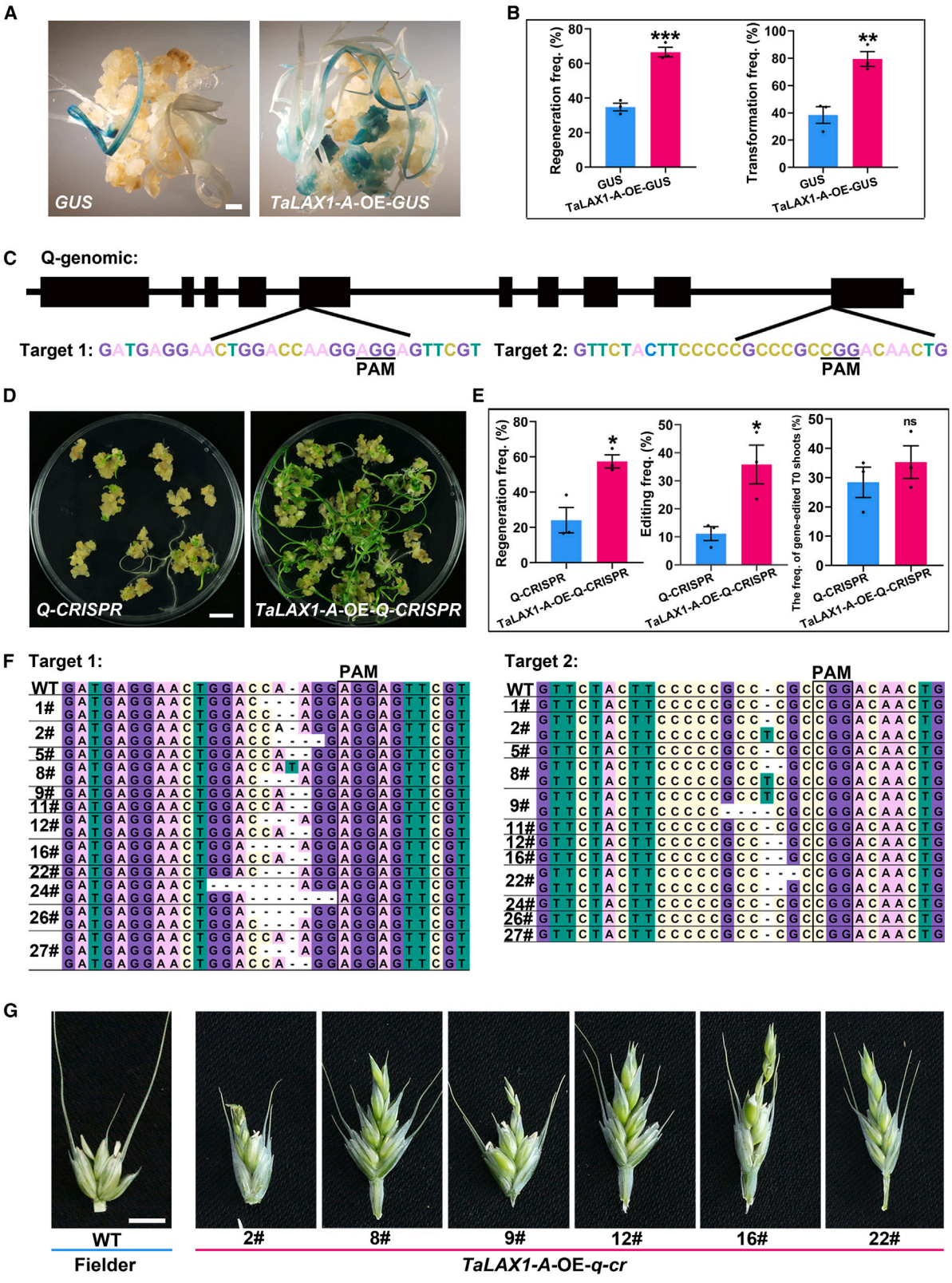

Figure 4. *TaLAX1-A* overexpression improves transformation and gene editing frequencies in the common wheat variety Fielder.

(A) Shoot regeneration and transformation phenotypes of immature embryos infected with the *Ubi*$_{pro}$*:GUS* (*GUS*) or *TaLAX1-A*-OE-*GUS* vector. Scale bar, 2 mm.

(B) Regeneration and transformation frequencies of immature embryos infected with the *GUS* or *TaLAX1-A*-OE-*GUS* vector.

(legend continued on next page)

TaLAX1-A promotes expression of *TaGRF* and *TaGIF* genes during wheat regeneration

To investigate the potential regulatory roles of *TaLAX1-A* during wheat regeneration, we performed RNA-sequencing (RNA-seq) analysis of Chinese Spring calli 5 days after transfer to shoot-induction medium. This specific stage was chosen because of the presence of morphologically regenerated shoot primordia (Supplemental Figure 6) and the highest *TaLAX1-A* expression during the shoot regeneration process (Supplemental Figure 2). Analysis of the RNA-seq data revealed 10 192 differentially expressed genes (DEGs) in *TaLAX1-A*-OE calli compared with the empty vector controls (Figure 5A). Among these DEGs, 5222 were upregulated, and 4970 were downregulated. The upregulated genes in *TaLAX1-A*-OE calli, which may be activated by *TaLAX1-A*, were enriched in functional annotations associated with cell proliferation, maintenance of shoot apical meristem identity, cytokinin biosynthetic process, and auxin responses and transport (Figure 5B). The downregulated genes in *TaLAX1-A*-OE calli were enriched in cytokinin metabolic process (Figure 5B).

In previous studies, overexpression of *TaGRF4* in combination with *TaGIF1* or *TaWOX5* has been shown to significantly increase regeneration efficiency in wheat and expand the number of transformable wheat genotypes (Debernardi et al., 2020; Wang et al., 2022a). Interestingly, the *TaGRF* genes and their co-factor, *TaGIF1*, were upregulated in *TaLAX1-A*-OE-transformed calli compared with the controls (Figure 5A). We further examined the transcript levels of these genes in *TaLAX1-A*-OE calli, which showed a substantial increase in *TaGRF* and *TaGIF1* expression (Figure 5C), supporting a role for TaLAX1-A in promoting expression of *TaGRFs* and *TaGIF1* during wheat regeneration. However, the transcript levels of *TaWOX5* did not differ significantly between *TaLAX1-A*-OE and control calli (Figure 5C).

To determine whether TaLAX1-A acts as a direct regulator of *TaGRF4* and *TaGIF1* transcription, we performed chromatin immunoprecipitation followed by quantitative polymerase chain reaction (ChIP–qPCR) experiments. We observed enrichment of specific fragments of the *TaGIF1-A* promoter (P2, −319 bp to −239 bp, and P4, −698 bp to −618 bp) (Figure 5D). By contrast, no enrichment of *TaGRF4-A* promoter fragment sequences was detected (Supplemental Figure 7). Luciferase activation assays further confirmed that TaLAX1-A binds directly to the *TaGIF1-A* promoter region and activates its expression (Figure 5E). Collectively, these findings strongly suggest that TaLAX1-A functions as a direct regulator of *TaGIF1* transcription during wheat regeneration, at least in part by binding to the *TaGIF1* promoter and enhancing *TaGIF1* expression, which may subsequently affect *TaGRF* activity.

TaLAX1-A overexpression enhances auxin response and cytokinin biosynthesis in wheat regeneration

Our transcriptomic analysis revealed significant upregulation of the *TaAUXIN RESPONSE FACTOR* (*TaARF*) genes *TaARF3*, *TaARF11*, *TaARF14*, and *TaARF15* and the auxin-transport-related *TaPINFORMED1* (*TaPIN*) genes *TaPIN1b* and *TaPIN1c* in *TaLAX1-A*-OE calli compared with controls (Figure 5A and 5C). We performed ChIP–qPCR and luciferase activation assays and found that TaLAX1-A binds to the promoter of *TaARF3-D*, which plays a crucial role in the plant regeneration process (Cheng et al., 2013), to activate its transcription (Figure 5F and 5G). IAA content did not differ significantly between the *TaLAX1-A*-OE transgenic calli and the controls (Figure 5H), suggesting that auxin biosynthesis may not be affected by TaLAX1-A overexpression. Transcription of cytokinin biosynthesis genes such as *TaISOPENTENYL TRANSFERASE 1* (*TaIPT1*), the *TaLONELY GUY* (*TaLOG*) genes *TaLOG1* and *TaLOG5*, and the *TaLONELY GUY-LIKE PROTEIN* (*TaLOGL*) genes *TaLOGL3*, *TaLOGL7*, *TaLOGL9*, and *TaLOGL10* was enhanced in *TaLAX1-A*-OE calli. Conversely, expression of the cytokinin metabolic process–related *TaCYTOKININ OXIDASE* (*TaCKX*) genes *TaCKX1*, *TaCKX2*, and *TaCKX4* was downregulated in *TaLAX1-A*-OE-transformed calli (Figures 5A, 5C, and 6A). We performed ChIP–qPCR and luciferase activation assays and found that TaLAX1-A binds to the *TaIPT1-A* promoter to activate its transcription (Figure 6B and 6C). This transcriptional activation was consistent with the significantly enhanced levels of endogenous cytokinin in the *TaLAX1-A*-OE transgenic calli (Figure 6D). These findings suggest that TaLAX1-A may play a role in regulating cytokinin accumulation by modulating the expression of genes related to cytokinin biosynthesis and metabolism, as well as influencing auxin responses and transport.

In PureWheat-mediated transformation, the presence of both auxin and cytokinin is necessary to induce callus formation and promote shoot regeneration (Ishida et al., 2015). Interestingly, in Fielder embryos inoculated with *Agrobacterium* carrying *TaLAX1-A*-OE, rapid shoot regeneration was observed even in medium without exogenously added cytokinin (Figure 6E and 6F and Supplemental Data 13). Moreover, the regeneration frequency upon *TaLAX1-A* overexpression in the absence of cytokinin was comparable to that of the empty vector control in medium containing cytokinin (Figures 1C and 6F and Supplemental Data 1 and 13). We next assessed the regeneration frequency and regenerating shoot frequency of immature Fielder embryos transformed with *TaLAX1-A*-OE or the empty vector in the absence of exogenous cytokinin and auxin. Regeneration frequency and regenerating shoot frequency were significantly higher in embryos transformed with *TaLAX1-A*-OE than in controls (Supplemental Figure 8 and Supplemental Data 14). Using the Ubi_{pro}*:GUS* vector, we compared the regeneration and

(C) Regions of the *Q* gene targeted with guide RNAs. PAM, protospacer-adjacent motif.

(D) Shoot regeneration phenotypes of immature embryos infected with the *Q-CRISPR* or *TaLAX1-A*-OE-*Q-CRISPR* vector. Scale bar, 1 cm.

(E) Regeneration frequencies, editing frequencies, and frequencies of gene-edited T0 shoots of immature embryos infected with the *Q-CRISPR* or *TaLAX1-A*-OE-*Q-CRISPR* vector. Editing frequency = no. of T0 plants with *Q* editing/no. of inoculated embryos × 100%. Frequency of gene-edited T0 shoots = no. of *Q*-gene-edited T0 plants/total no. of T0 plants × 100%.

(F) Twelve transgenic T0 plants with *Q*-edited genomic sequences. The 2#, 8#, 9#, 12#, 16#, and 22# lines carry two target mutations.

(G) Edited T0 plants showing increased numbers of florets per spikelet. Scale bar, 0.5 cm. Values in **(B)** and **(E)** are means ± SEM from three independent experiments. Black points are the results from individual experiments. ***$P < 0.001$; **$P < 0.01$; *$P < 0.05$; ns, not significant (Student's *t*-test, two-tailed).

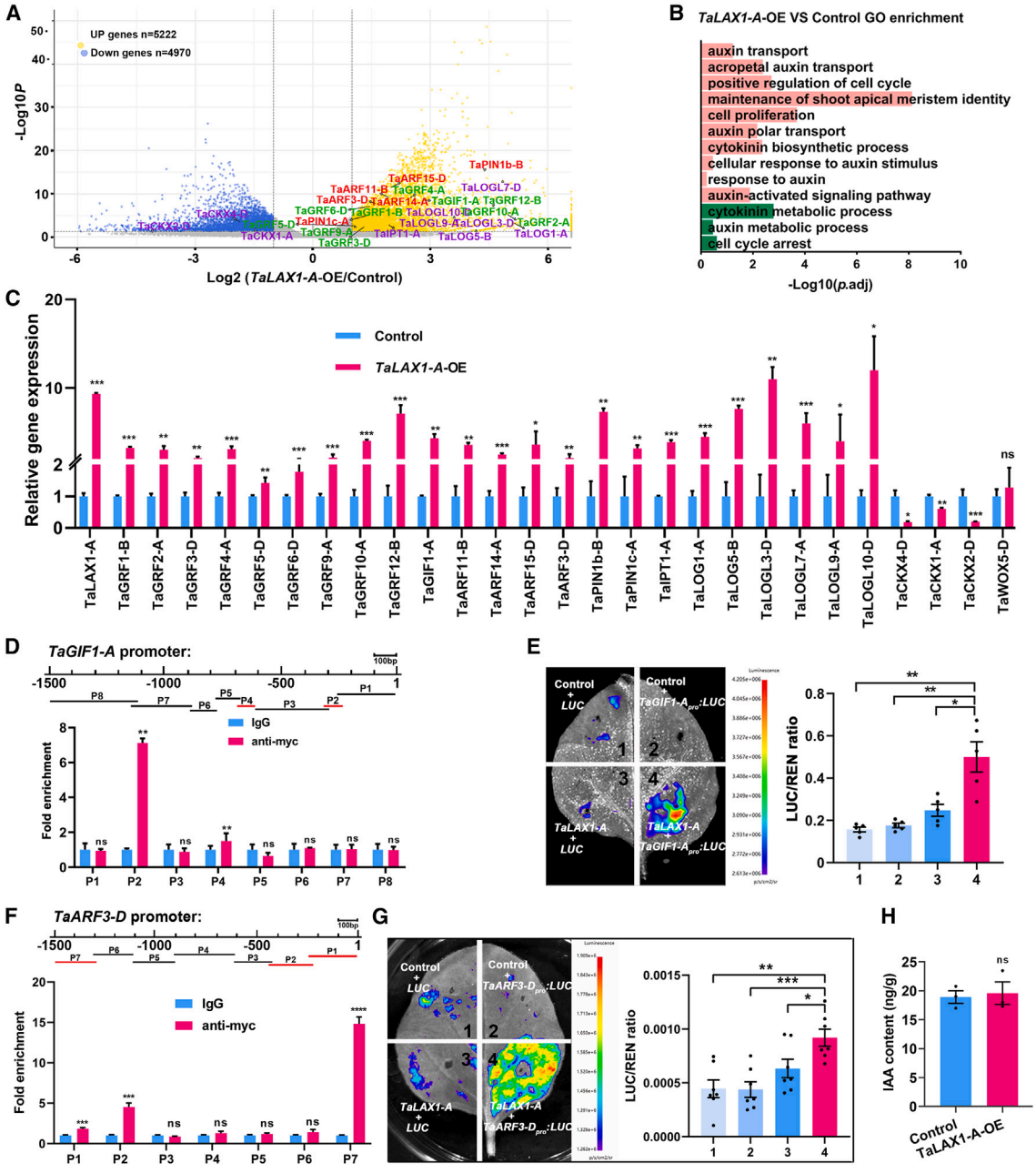

Figure 5. RNA-seq analysis of *TaLAX1-A*-OE transgenic calli and activation of *TaGIF1-A* and *TaARF3-D* by TaLAX1-A.

(A) Volcano plot of up- and downregulated genes in *TaLAX1-A*-OE transgenic calli vs. empty vector (control) transgenic calli of Chinese Spring. Purple, cytokinin-related genes; red, auxin-related genes; green, *TaGRFs* and *TaGIF1-A*.

(B) Gene Ontology (GO) enrichment analysis of up- and downregulated genes from *TaLAX1-A*-OE transgenic calli vs. empty vector (control) transgenic calli. Red, GO terms of genes upregulated in *TaLAX1-A*-OE vs. control; green, GO terms of genes downregulated in *TaLAX1-A*-OE vs. control.

(C) Relative expression levels of selected genes regulated by TaLAX1-A in *TaLAX1-A*-OE transgenic calli and empty vector transgenic calli.

(D) ChIP–qPCR of the *TaGIF1-A* promoter using an anti-*myc* antibody in the *TaLAX1-A*-OE transgenic lines. *TaLAX1-A*-OE samples with IgG antibody were used as negative controls. TaLAX1-A binds to the P2 and P4 regions of the *TaGIF1-A* promoter.

(E) Transient expression of TaLAX1-A protein and *TaGIF1-A*$_{pro}$*:LUC* reporter in tobacco leaves (left) and statistics of luciferase activity (right).

(F) ChIP–qPCR of the *TaARF3-D* promoter using an anti-*myc* antibody in the *TaLAX1-A*-OE transgenic lines; *TaLAX1-A*-OE samples with IgG antibody were used as a negative control. TaLAX1-A binds to the P1, P2, and P7 regions of the *TaARF3-D* promoter.

(G) Transient expression of TaLAX1-A protein and *TaARF3-D*$_{pro}$*:LUC* reporter in tobacco leaves (left) and statistics of luciferase activity (right).

(H) Endogenous IAA content in *TaLAX1-A*-OE transgenic calli and empty vector (control) transgenic calli. Values in **(C)**, **(D)**, and **(F)** are means ± SD; values in **(E)**, **(G), and (H)** are means ± SEM. All experiments were performed at least three times. Black points are the results from individual experiments. ****$P < 0.0001$; ***$P < 0.001$; **$P < 0.01$; *$P < 0.05$; ns, not significant (Student's *t*-test, two-tailed).

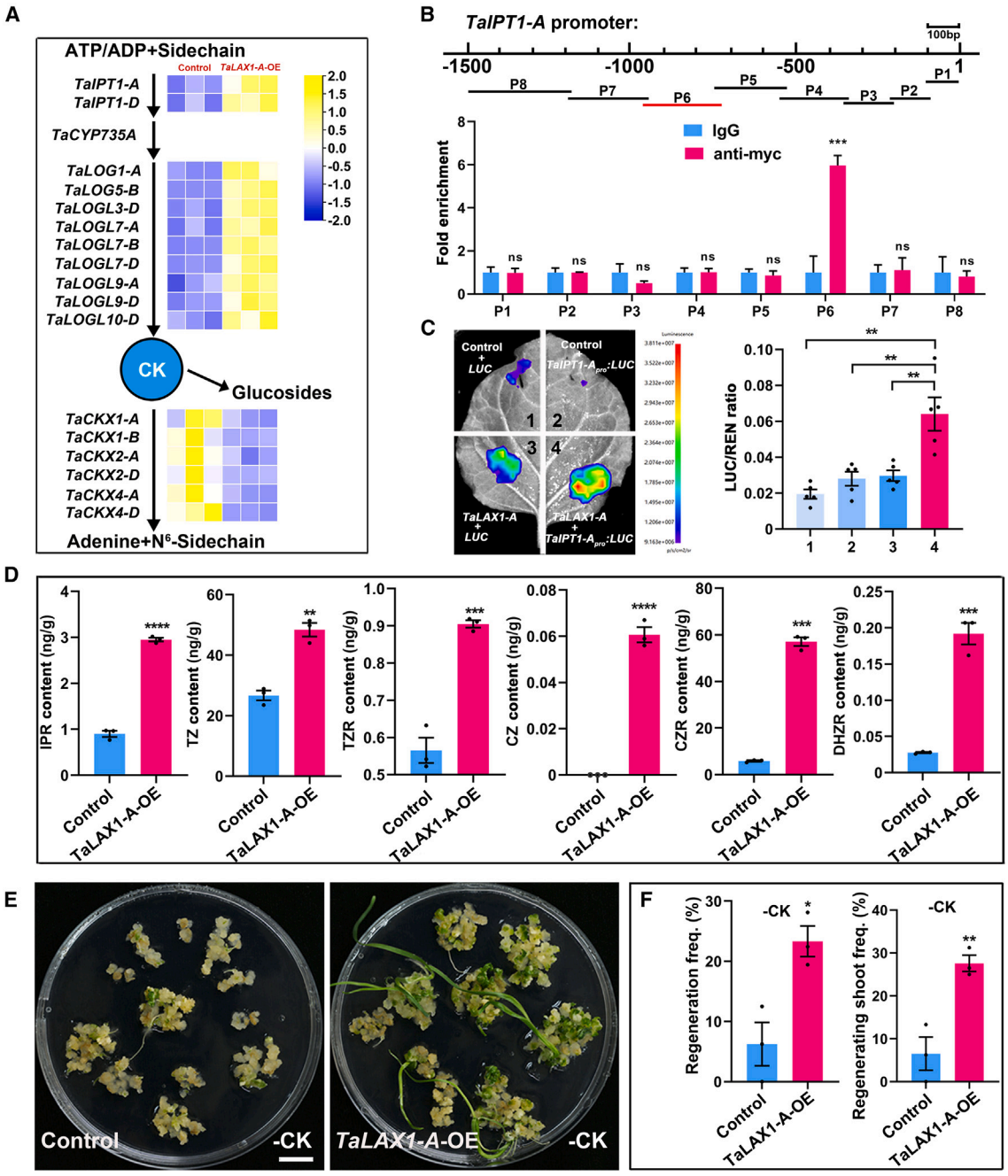

Figure 6. TaLAX1-A activates cytokinin biosynthesis during the process of shoot regeneration.

(A) Expression heatmap of genes related to cytokinin biosynthetic and metabolic processes in control (empty vector) transgenic calli and *TaLAX1-A*-OE transgenic calli.

(B) ChIP–qPCR of the *TaIPT1-A* promoter using an anti-*myc* antibody in the *TaLAX1-A*-OE transgenic lines; *TaLAX1-A*-OE samples with IgG antibody were used as a negative control. TaLAX1-A binds to the P6 region of the *TaIPT1-A* promoter.

(C) Transient expression of TaLAX1-A protein and *TaIPT1-A$_{pro}$:LUC* reporter in tobacco leaves (left) and statistics of luciferase activity (right).

(D) Endogenous cytokinin content (IPR, TZ, TZR, CZ, CZR, and DHZR) in *TaLAX1-A*-OE transgenic calli and empty vector (control) transgenic calli.

(E) Shoot regeneration phenotypes of Fielder embryos transformed with the empty vector (control) or *TaLAX1-A*-OE after incubation on CIM for 42 days and then on SIM (without exogenous cytokinin) for 20 days. Scale bar, 1 cm.

(F) Regeneration frequencies and regenerating shoot frequencies of Fielder immature embryos infected with control or *TaLAX1-A*-OE after incubation on CIM for 42 days and then on SIM (without exogenous cytokinin) for 20 days. Values in **(B)** are means ± SD; values in **(C)**, **(D)**, and **(F)** are means ± SEM. All experiments in **(B)–(D)** and **(F)** were performed at least three times. Black points are the results from individual experiments. $^{****}P < 0.0001$; $^{***}P < 0.001$; $^{**}P < 0.01$; $^{*}P < 0.05$; ns, not significant (Student's *t*-test, two-tailed).

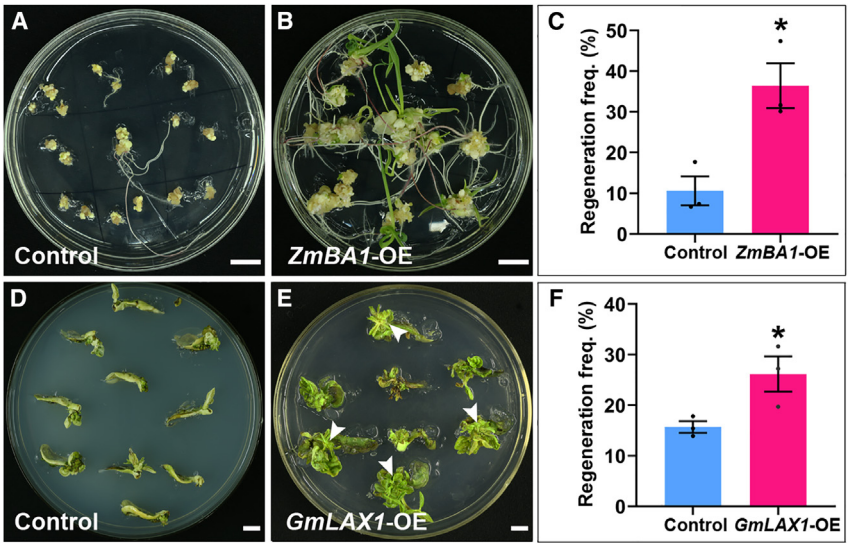

Figure 7. Transformation of *TaLAX1* homologs into maize and soybean.

(A) Shoot regeneration phenotypes of maize (B104) transformed with the empty vector (control, p3300-CUB). Scale bar, 1 cm.

(B) Shoot regeneration phenotypes of maize (B104) transformed with *ZmBA1*-OE. Scale bar, 1 cm.

(C) Regeneration frequencies of B104 immature embryos infected with control or *ZmBA1*-OE. Regeneration frequency = no. of calli showing at least one regenerating shoot/no. of inoculated embryos × 100%.

(D) Shoot regeneration phenotypes of soybean (Dongnong-50) transformed with the empty vector (control, 35S-PBI106). Scale bar, 1 cm.

(E) Shoot regeneration phenotypes of soybean (Dongnong-50) transformed with *GmLAX1*-OE. Regenerated shoots are indicated with white arrows. Scale bar, 1 cm.

(F) Regeneration frequencies of Dongnong-50 cotyledonary nodes infected with control or *GmLAX1*-OE. Regeneration frequency = no. of explants showing at least one regenerating shoot/no. of inoculated explants × 100%. Values in **(C)** and **(F)** are means ± SEM from three independent experiments. Black points are the results from individual experiments. $^*P < 0.05$ (Student's *t*-test, two-tailed).

transformation frequencies of stable *TaLAX1-A*-OE T1 transgenic lines and non-transgenic lines in the absence of cytokinin or in the absence of both cytokinin and auxin. Under these conditions, the regeneration and transformation frequencies of *TaLAX1-A*-OE T1 transgenic plants were significantly higher than those of the non-transgenic lines (Supplemental Figures 9 and 10 and Supplemental Data 15 and 16). These results suggest that *TaLAX1-A* overexpression can promote shoot regeneration and partially compensate for a lack of exogenous cytokinin and auxin supplementation.

TaLAX1 homologs in maize and soybean promote shoot regeneration

To investigate the potential of *TaLAX1* homologs to promote transformation efficiency in other crop species, we examined their effects in the monocot maize and the dicot soybean. Transformation of both maize and soybean is currently limited to a narrow range of genotypes (Jia et al., 2015; Lowe et al., 2016; Wang et al., 2022a, 2022b). Through phylogenetic analysis, we identified *ZmBA1* in maize and *GmLAX1* in soybean as homologs of wheat *TaLAX1* (Supplemental Figure 1A). Overexpression of *ZmBA1* significantly increased the regeneration frequency of maize B104 lines from 10.59% ± 3.55% to 36.40% ± 5.52% (Figure 7A–7C and Supplemental Data 17). Similarly, overexpression of *GmLAX1* in the soybean variety Dongnong-50 significantly increased regeneration frequency from 15.68% ± 1.08% to 26.18% ± 3.48% (Figure 7D–7F and Supplemental Data 18). We performed further cultivation of the regenerated shoots derived from immature maize embryos transformed with *ZmBA1*-OE and soybean cotyledonary nodes transformed with *GmLAX1*-OE, and these regenerated shoots successfully developed into complete plants (Supplemental Figure 11A and 11C). Several of these plants were identified as overexpression lines through real-time qPCR analyses (Supplemental Figure 11B and 11D). These findings demonstrate that *TaLAX1* homologs positively enhance regeneration in the monocot and dicot species tested in this study. Therefore, we propose that the benefits of *LAX1* technology may be extended to improve transformation efficiency in other crop varieties.

DISCUSSION

Wheat *TaLAX1* exhibits homology to *OsLAX1* in rice and *ZmBA1* in maize, based on their amino acid sequence similarities (Komatsu et al., 2003; Gallavotti et al., 2004). In rice, strong alleles of *lax1* mutants display severe defects in initiation of lateral spikelets and panicle branches (Komatsu et al., 2003). Similarly, maize mutants with the *ba1* allele fail to initiate lateral meristems during both vegetative and reproductive development, resulting in unbranched, short, and sterile tassels without spikelets (Ritter et al., 2002; Gallavotti et al., 2004; Skirpan et al., 2008; Yao et al., 2019). However, wheat *Talax1-aabbdd* mutants exhibit a compact spike phenotype (He et al., 2021), which is distinct from the reduced lateral branching observed in rice *lax1* and maize *ba1* mutants. These different phenotypes indicate that rice and maize homologs have undergone functional diversification. In this study, we revealed a novel role for *TaLAX1* in the regulation of wheat regeneration and transformation. These proteins and their homologs show potential as enhancers to improve genetic transformation and genome editing efficiency in various crop species.

The low regeneration capability and genotype-specific growth requirements of explant embryos have posed challenges to achieving high transformation efficiency in wheat. Despite efforts to develop efficient transformation protocols, many wheat varieties, including Aikang 58 and Jimai 22, remain recalcitrant to existing methods (Wang et al., 2017, 2022a). Susceptibility to *Agrobacterium* infection and efficiency of regeneration often exhibit notable genotype specificity, limiting the applicability of transformation protocols to only a few wheat genotypes (Wang et al., 2017, 2022a). Recent studies using multiomics data have uncovered a transcriptional regulatory network involved in wheat regeneration, highlighting the sequential expression of

genes responsible for cell fate reprogramming, which is triggered by auxin and coordinated with changes in chromatin accessibility and histone modifications (Liu et al., 2023). Several wheat factors involved in developmental reprogramming have been identified as critical regulators that can transform somatic cells into embryogenic cells, and these factors have been designated "boosters" for regeneration efficiency in transformed wheat embryos. Overexpression of these boosters, such as the fusion protein TaGRF4–TaGIF1 or TaWOX5, has been shown to enhance regeneration efficiency with reduced dependence on specific genotypes (Debernardi et al., 2020; Wang et al., 2022a; Qiu et al., 2022).

Interestingly, we also observed that overexpression of *TaLAX1* significantly improved transformation efficiency in wheat. Transgenic plants overexpressing *TaLAX1* were fertile and did not exhibit obvious developmental or reproductive defects. These findings distinguish *TaLAX1* from other regeneration-related factors that may introduce additional plant phenotypes, which can pose challenges in certain experimental applications. Furthermore, *TaLAX1-A* overexpression enhances regeneration efficiency in previously recalcitrant wheat varieties such as Aikang 58 and Jimai 22. These varieties, known for their low regeneration efficiency, have been difficult to transform and genome edit using existing methods. Therefore, the introduction of *TaLAX1-A* overcomes such genotype limitations and expands the available resources for transformation.

The process of shoot regeneration in a wide variety of crops relies on the addition of appropriate plant hormones, particularly auxin and cytokinin, to the regeneration medium. Targeted manipulation of hormone signaling pathways has been shown to activate the accumulation of auxin and cytokinin, enhancing shoot regeneration even in recalcitrant crop varieties (Paek and Hahn, 2000; Cheng et al., 2013; Ishida et al., 2015; Li et al., 2017b; Meng et al., 2017). In our study, we collected calli for transcriptomic analysis 5 days after transfer to shoot induction medium because this stage is likely critical for shoot apical meristem formation: morphologically regenerated shoot primordia are present, and the highest *TaLAX1* expression is observed at this stage. Through RNA-seq analysis, we identified significant upregulation of auxin response genes (*TaARFs*), auxin transport genes (*TaPINs*), and cytokinin biosynthesis genes (*TaIPT1*, *TaLOGs*, and *TaLOGLs*) in *TaLAX1-A*-overexpressing transformed tissues. Consistent with these findings, endogenous cytokinin levels were significantly higher in *TaLAX1-A*-overexpressing calli than in controls. Furthermore, Fielder embryos infected with the *TaLAX1-A*-OE vector were able to rapidly regenerate green shoots when cultured in medium without cytokinin, confirming that *TaLAX1-A* promotes endogenous cytokinin accumulation. Moreover, we found that TaLAX1-A directly binds to the promoter regions of both *TaIPT1-A* and *TaARF3-D* to activate their transcription. These findings suggest that TaLAX1-A may play a role in regulating shoot regeneration by modulating cytokinin biosynthesis and metabolism, as well as auxin responses and transport.

Even in the absence of exogenous cytokinin and auxin, the calli derived from Fielder embryos infected with the empty vector retained some regenerative capacity. This finding could be attributed to the intrinsic regenerative ability of the Fielder genotype, which has shown stronger regenerative capacity than other genotypes used in the PureWheat technique (Wang et al., 2017; Debernardi et al., 2020). In addition, the cutting processes involved in the regeneration protocol may induce wounding signals that trigger callus and shoot formation, leading to accumulation of hormones such as auxin, cytokinin, and jasmonate, which promote plant regeneration (Ikeuchi et al., 2017; Zhang et al., 2019). Transcriptional regulators such as ETHYLENE RESPONSE FACTOR 115 (ERF115), WOUND-INDUCED DEDIFFERENTIATION1 (WIND1), ENHANCER OF SHOOT REGENERATION 1 (ESR1), PLETHORA3 (PLT3), PLT5, and PLT7 are also upregulated by wounding and play a role in promoting plant regeneration (Ikeuchi et al., 2017; Iwase et al., 2017; Chen et al., 2022).

We found that *TaGRFs* and *TaGIF1* were upregulated by *TaLAX1-A* overexpression and that TaLAX1-A directly regulated the expression of *TaGIF1*. These results indicate that TaLAX1-A may regulate shoot regeneration through the same pathway as TaGRF4–TaGIF1, suggesting a regulatory network involving auxin, cytokinin, and related transcription factors like TaGRFs and TaGIF1, which are responsible for cell division, cell fate transition, and ultimate shoot regeneration.

Compared with the gene combinations of *BBM–WUS2* and *GRF4–GIF1*, overexpression of a single gene, *LAX1*, significantly increased crop regeneration frequency. Moreover, transgenic plants overexpressing *LAX1* were fertile and did not exhibit obvious developmental or reproductive defects. These findings distinguish LAX1 from other regeneration-related factors that may introduce additional plant phenotypes, which could pose challenges in certain experimental applications. Thus, combining LAX1 technology with other approaches such as "altruistic transformation" (Hoerster et al., 2020) or the use of conditional expression drivers (Lowe et al., 2018; Gao et al., 2020) is recommended to avoid such effects. Another strategy involves linking regeneration-promoting gene elements with the CRISPR–Cas9 system (Gao et al., 2016; Lu et al., 2017; Chen et al., 2019).

In conclusion, the regeneration step is the main bottleneck for efficient transformation and genome editing in wheat. Previous studies have attempted to enhance transformation efficiency in wheat by making use of genes that promote regeneration during tissue culture (Debernardi et al., 2020; Wang et al., 2022a; Qiu et al., 2022). However, effective methods for regenerating transformed somatic cells into whole plants are still limited. In our study, we discovered that overexpression of *TaLAX1* significantly increases regeneration efficiency in certain wheat varieties. Our findings demonstrate that this increased efficiency is associated with the upregulation of *TaGRF and TaGIF* genes, as well as genes related to auxin response and transport and cytokinin biosynthesis. Overexpression of *TaLAX1* homologs also improved the formation of transgenic plants in soybean and maize, suggesting that *TaLAX1* may be a promising strategy for overcoming the transformation barrier in economically important crops.

METHODS

Plant materials and growth conditions

The hexaploid wheat varieties used in the present work included Fielder, Chinese Spring, Kenong 199, Shannong 28, Jimai 22, and Aikang 58. The tetraploid wheat varieties used were Langdon and Kronos. Fielder

seeds were generously provided by Japan Tobacco. All wheat varieties used in the regeneration and transformation experiments were grown in growth chambers under long-day conditions (16-h light/8-h dark) at 22°C. Facultative or winter varieties were maintained at 4°C for 30 days for vernalization before being transplanted to soil. Plants used for growth and developmental phenotype analyses were planted at the experimental station of Shandong Agricultural University (E 117°, N 36°).

Plasmid construction

We generated the PC186-*TaLAX1-myc* construct using the Gateway system (Invitrogen, Carlsbad, CA, USA). The sequence of myc and several restriction enzyme cutting sites (GCGGCCGCatggaacagaaactgatctctga agaagatctgGAATTCCATATGGGATCCCTGCAGGGTACCATCAGTAAGC TTCCATGGGAGCTCATCGATGTCGACTCTAGACTCGAGGGCGCGCC) was synthesized and inserted into the pENTR vector to generate the *myc-mcs*-ENTR vector. The *TaLAX1-A/B/D* genomic sequences were amplified using 2×Phanta Max Master Mix (Vazyme, Nanjing, China; P515-01) and inserted into the *myc-mcs*-ENTR vector between *Eco*RI and *Hind*III. *myc-TaLAX1*-ENTR was then recombined into the PC186 vector through Gateway LR recombination. For the *TaLAX1-A*-OE-*GUS* construct, we amplified the Nos terminator from the PC186 plasmid and inserted it into the *myc-TaLAX1-A*-ENTR vector between *Sac*I and *Cla*I. The Ubi_{pro}*:GUS* module was amplified from the Ubi_{pro}*:GUS* plasmid and inserted into the *myc-TaLAX1-A-Nos Terminator*-ENTR vector between *Xho*I and *Xba*I, and *myc-TaLAX1-A-Nos Terminator-*Ubi_{pro}*:GUS*-ENTR was then recombined into the PC186 vector through Gateway LR recombination.

To generate the *TaLAX1-A-CRISPR* and *Q-CRISPR* constructs, two single-guide RNA sequences were designed to target the *TaLAX1-A* promoter and the coding sequence of the *Q* gene. In accordance with the methods described by Xing et al. (2014), the single-guide RNAs were inserted into the PBUE413 vector. To generate the *TaLAX1-A*-OE-*Q-CRISPR* construct, Ubi_{pro}*:TaLAX1-A-Nos Terminator* synthetic fragments were digested with *Pme*I and then inserted into the *Q-CRISPR* vector.

To generate the *ZmBA1*-OE construct, we amplified the *ZmBA1* genomic sequence and inserted it into the p3300-CUB vector (Cambia) between *Sma*I and *Sac*I. To produce the *GmLAX1*-OE construct, we amplified the 35S promoter sequence from the PROK II vector and inserted it into the PBI106 vector between *Eco*RI and *BamH*I. *GmLAX1* genomic sequences were then amplified and inserted into the 35S-PBI106 vector between *Xho*I and *Sac*I. The primers used for plasmid construction are listed in Supplemental Data 19.

Plant transformation

To perform wheat transformation, we obtained immature embryos (approximately 14 days post anthesis) from the indicated wheat lines. The transformation procedure followed the protocols outlined in a previous study (Ishida et al., 2015). The *Agrobacterium tumefaciens* strain EHA105 was used to introduce the PC186-*TaLAX1-myc*, PC186 empty vector, *TaLAX1-A*-OE-*GUS*, Ubi_{pro}*:GUS*, *TaLAX1-A-CRISPR*, *TaLAX1-A*-OE-*Q-CRISPR*, and *Q-CRISPR* vectors into the immature embryos. After *Agrobacterium* infection, the immature embryos were initially cultured on WLS-AS medium (1/100 volume of 10× LS major salts, 1/1000 volume of 100× FeEDTA, 1/1000 volume of 100× LS minor salts, 1/1000 volume of 100× MS vitamins, 8 g/l agarose, 10 mg/l glucose, 0.5 g/l MES, 0.85 mg/l $AgNO_3$, 100 μM AS, 1.25 mg/l $CuSO_4 \cdot 5H_2O$) for 2 days. The embryo axis was then excised from the embryos and transferred to WLS-Res medium (1/10 volume of 10× LS major salts, 1/100 volume of 100× FeEDTA, 1/10 volume of 100× LS minor salts, 0.5 mg/l 2,4-D, 1/100 volume of 100× MS vitamins, 2.2 mg/l picloram, 0.75 g/l $MgCl_2 \cdot 6H_2O$, 0.5 g/l glutamine, 0.1 g/l casein hydrolysate, 40 g/l maltose, 1.95 g/l MES, 5 g/l agarose, 250 mg/l carbenicillin, 100 mg/l ascorbic acid, 0.85 mg/l $AgNO_3$, 100 mg/l cefotaxime) for 5 days. The explants were next moved to WLS-P5 medium (1/10 volume of 10× LS major salts, 1/100 volume of 100× FeEDTA, 0.5 mg/l 2,4-D, 1/10 volume of 100× LS minor salts, 1/100 volume of 100× MS vitamins, 2.2 mg/l picloram, 0.1 g/l casein hydrolysate, 0.5 g/l glutamine, 0.75 g/l $MgCl_2 \cdot 6H_2O$, 5 g/l agarose, 40 g/l maltose, 1.95 g/l MES, 100 mg/l ascorbic acid, 250 mg/l carbenicillin, 5 mg/l phosphinothricin, 0.85 mg/l $AgNO_3$) and cultured for 14 days. Each explant was then divided into two parts and transferred to WLS-P10 medium (WLS-P5 supplemented with 5 mg/l phosphinothricin) for 21 days to induce callus formation. The proliferated calli were transferred to LSZ-P5 medium (1/10 volume of 10× LS major salts, 1/100 volume of 100× FeEDTA, 1/100 volume of 100× LS minor salts, 20 g/l sucrose, 1/100 volume of 100× modified LS vitamins, 5 mg/l zeatin, 0.5 g/l MES, 2.5 mg/l $CuSO_4 \cdot 5H_2O$, 250 mg/l carbenicillin, 8 g/l agar, 100 mg/l cefotaxime, 5 mg/l phosphinothricin) to induce shoot regeneration. The regenerated shoots were transferred to LSF-P5 medium (1/10 volume of 10× LS major salts, 1/100 volume of 100× FeEDTA, 1/100 volume of 100× LS minor salts, 0.5 g/l MES, 1/100 volume of 100× modified LS vitamins, 15 g/l sucrose, 3 g/l Gelrite, 0.2 mg/l IBA, 250 mg/l carbenicillin, 5 mg/l phosphinothricin) until root elongation. In this study, the abbreviations used for the respective media were CIM (callus induction medium) for WLS-AS, WLS-Res, WLS-P5, and WLS-P10 and SIM (shoot induction medium) for LSZ-P5.

To perform maize transformation, *ZmBA1*-OE and p3300-CUB empty vectors were transformed into *A. tumefaciens* EHA105. Immature maize zygotic embryos (12 days after pollination) from the inbred line B104 were used for *Agrobacterium*-mediated transformation according to a previously described protocol (Frame et al., 2011) with slight modifications. In brief, the infected immature embryos were initially cultured on co-cultivation medium (0.7 g/l L-proline, 4.3 g/l MS salts, 100 mg/l casein hydrolysate, 0.5 ml/l dicamba, 100 mg/l myo-inositol, 2.3 g/l Gelrite, 30 g/l sucrose, 1 ml/l MS vitamin stock, 88 mM silver nitrate, 100 mM AS, 300 mg/l L-cysteine). After 16 h, the explants were transferred to selection medium (0.7 g/l L-proline, 0.5 g/l MES, 4.3 g/l MS salts, 100 mg/l casein hydrolysate, 0.5 ml/l dicamba, 30 g/l sucrose, 100 mg/l myo-inositol, 2.3 g/l Gelrite, 1 ml/l MS vitamin stock, 88 mM silver nitrate, 250 mg/l carbenicillin, 1 mg/l bialaphos) for 14 days. The explants were then transferred to regeneration medium (1 ml/l modified MS vitamin stock, 4.3 g/l MS salts, 60 g/l sucrose, 100 mg/l myo-inositol, 3 g/l Gelrite, 6 mg/l glufosinate ammonia, 100 mg/l cefotaxime) for 4–8 weeks, with regular transfers to fresh regeneration medium every 2 weeks. The regenerated shoots were transferred to rooting medium (1 ml/l modified MS vitamin stock, 4.3 g/l MS salts, 30 g/l sucrose, 100 mg/l myo-inositol, 3 g/l Gelrite, 6 mg/l glufosinate ammonia, 100 mg/l cefotaxime) until root elongation.

For soybean transformation, *GmLAX1*-OE and PBI106 empty vectors were introduced into Dongnong-50 using *Agrobacterium* (EHA105)-mediated genetic transformation of soybean cotyledonary nodes as described in a previous study (Li et al., 2017b). Cotyledonary node explants were infected with *Agrobacterium* and placed on co-cultivation medium (3.9 g/l B5 salts, 30 g/l sucrose, 3.9 g/l MES, 8 g/l agar powder, 400 mg/l cysteine, 154.2 mg/l DTT, 0.25 mg/l GA_3, 1.67 mg/l 6-BA, 40 mg/l AS) for 3 days. The explants, with hypocotyls removed, were then cultured in shoot induction medium (3.9 g/l B5 salts, 30 g/l sucrose, 0.59 g/l MES, 8 g/l agar powder, 1.67 mg/l 6-BA, 250 mg/l Timentin, 100 mg/l cefotaxime, 45 mg/l kanamycin). After 14 days, the explants were transferred to fresh shoot induction medium without kanamycin. After 28 days of cultivation in shoot induction medium, explants with regenerated shoots were transferred to shoot elongation medium (4.3 mg/l MS, 30 g/l sucrose, 0.59 g/l MES, 8 g/l agar powder, 50 mg/l asparagine, 50 mg/l L-pyroglutamic acid, 0.1 mg/l IAA, 0.5 mg/l GA_3, 1 mg/l zeatin-R, 250 mg/l Timentin, 100 mg/l cefotaxime) and cultured for 4 weeks. Finally, the regenerated shoots were transferred to rooting medium (4.3 mg/l MS, 30 g/l sucrose, 0.59 g/l MES, 8 g/l agar powder, 50 mg/l asparagine, 50 mg/l L-pyroglutamic acid) and cultured for 2 weeks to produce complete plants.

Regenerative phenotype calculations

In wheat, callus proliferation frequency was determined by measuring the weights of immature embryos cultured on CIM for 42 days. The regeneration frequencies, regenerating shoot frequencies, transformation frequencies, gene editing frequencies, and frequencies of gene-edited T0 shoots were calculated after the immature embryos had been cultured on CIM for 42 days and then on SIM for 20 days. For the calculation of regenerated shoots, only those >2 cm in length were considered, as they exhibited a higher potential for development into fully grown seedlings and plants compared with smaller shoots.

In maize, regeneration frequencies of elongated regenerating shoots were calculated before transfer to root induction medium. Only shoots >2 cm were considered and included in the calculation.

In soybean, regeneration frequencies were determined after the explants had been cultured on shoot induction medium for 28 days. Only shoots >2 cm were considered for the calculation, with particular emphasis on identifying regenerated shoots that possessed a shoot meristem.

Total RNA isolation and real-time qPCR analysis

We extracted total RNA from the indicated tissues using the CWBio Ultrapure RNA Kit. The FastKing RT Kit (Tiangen Biotech, Beijing, China) was used to synthesize first-strand cDNA. SYBR Green Real-Time PCR Master Mix (Tiangen Biotech) was used to perform qPCR analysis. We used the SYBR Green Master Mix to dilute each cDNA. Relative transcript levels were normalized to that of *TaACTIN*, *ZmACTIN*, or *GmACTIN*. All measurements were carried out with three biological replicates. We used the comparative C_T method to determine expression values. The primers used for qPCR analysis are listed in Supplemental Data 19.

Transcriptome analysis

For transcriptome sequencing, we collected calli induced from *de novo*-transformed immature embryos transformed with the empty vector or *TaLAX1-A*-OE and cultured on CIM for 42 days and SIM for 5 days. Transcriptomics analysis was performed using previously described protocols (Li et al., 2021). Three independent biological replicates were performed for each specimen; sequencing was performed by OE Biotech (Shanghai, China). Clean reads were mapped to the wheat genome (version IWGSC RefSeq 1.1). Genes with a greater than two-fold expression change and a false discovery rate of less than 0.05 were considered to be DEGs.

RNA *in situ* hybridization

TaLAX1-A cDNA was amplified and ligated into the pEasy-Blunt3 vector, and the insertion direction of the fragments was verified by sequencing. RNA *in situ* hybridization was performed with digoxigenin-labeled sense and antisense probes on 8-μm sections of the indicated tissues as described previously (Su et al., 2020).

GUS staining

Specimens were placed in GUS staining solution (10 mM EDTA, 1 mM 5-bromo-4-chloro-3-indolyl-b-D-glucuronic acid, 3 mM each $K_3Fe(CN)_6$/$K_4Fe(CN)_6$, 100 mM Na_3PO_4 buffer, and 0.1% Nonidet P-40) and incubated at 37°C overnight. After staining, we used 95% ethanol to remove chlorophyll.

Chromatin immunoprecipitation analysis

TaLAX1-A-OE lines (15 days old) were harvested for ChIP analysis according to previously described protocols (Li et al., 2017a) with minor modifications. The DNA fragments combined with TaLAX1-A protein were co-immunoprecipitated using anti-*myc* antibody (1:500, 06-340; Sigma-Aldrich). *TaLAX1-A*-OE samples with IgG antibody (1:500, 12-371; Merck) were used as negative controls. For each ChIP assay, we performed three biological repeats. All primers used for the ChIP assays are listed in Supplemental Data 19.

Luciferase assay

The 1500-bp *TaGIF1-A*, *TaIPT1-A*, and *TaARF3-D* promoters were individually fused with the luciferase reporter gene via the *Xho*I and *BamH*I sites of the pGreenII 0800-LUC vector (Hellens et al., 2005). The coding region of the *TaLAX1-A* gene was fused to the pGreenII 62-SK vector downstream of the 35S promoter between the *BamH*I and *Xho*I sites. The resulting plasmids were transformed into *A. tumefaciens* strain EHA105. *Nicotiana benthamiana* leaves were infiltrated with different mixed combinations of *Agrobacterium* and collected for transient transcription assays as described previously (Su et al., 2020).

Quantification of cytokinin

We collected calli induced from immature embryos that had been transformed with the empty vector or *TaLAX1-A*-OE and cultured on CIM for 42 days. Endogenous cytokinin levels were measured by Wuhan Greensword Creation Technology using LC–MS/MS analysis as reported previously (Liu et al., 2010).

Free IAA measurements

Calli induced from immature embryos that had been transformed with the empty vector or *TaLAX1-A*-OE and cultured on CIM for 11 days were collected for free IAA measurements. Free IAA measurements were performed as reported previously (Li et al., 2021).

Sequence alignment and phylogenetic analysis

We used MEGA 11 to perform sequence alignment and construct a phylogenetic tree of OsLAX1 and its homologous proteins in the indicated species using the neighbor-joining method and 1000 bootstrap replicates.

Paraffin sections

Chinese Spring materials were collected at various stages of wheat regeneration during tissue culture. The specimens were preserved by immersion in a 4% glutaraldehyde solution at 4°C overnight. The fixed specimens were then dehydrated in a series of ethanol concentrations ranging from 10% to 100%. After an 8-h xylene treatment, the samples were immersed in liquid paraffin for 3–5 days and then fixed in paraffin blocks. Sections (8 μm) were stained with toluidine blue O (T3260; Sigma-Aldrich) for 1 min.

Statistical analysis

Statistical analyses were performed with GraphPad Prism 8. All data were analyzed using Student's *t*-test (two-tailed) or one-way ANOVA with Tukey's multiple comparisons test, and $P < 0.05$ was considered significant.

Data and code availability

The RNA-seq data discussed in this study have been deposited at the National Genomics Data Center Genome Sequence Archive (GSA; https://ngdc.cncb.ac.cn/gsa/) under accession no. CRA008766. All source data for the statistics shown in the figures are provided in Supplemental Data 1–19. Gene sequence data mentioned in this study can be found at EnsemblPlants (https://plants.ensembl.org/index.html) under the following accession numbers: *TaLAX1-A* (*TraesCS3A02G350600*), *TaLAX1-B* (*TraesCS3B02G383000*), *TaLAX1-D* (*TraesCS3D02G344600*), *ZmBA1* (*Zm00001d042989*), *GmLAX1* (*GLYMA_18G204700*), *Q* (*TraesCS5A01G473800*), *TaGIF1-A* (*TraesCS4A02G250600*), *TaGRF4-A* (*TraesCS6A02G269600*), *TaIPT1-A* (*TraesCS1A02G376300*), and *TaARF3-D* (*TraesCS3D02G292100*).

SUPPLEMENTAL INFORMATION

Supplemental information is available at *Plant Communications Online*.

FUNDING

This research was funded by the National Key Research and Development Program of China (2022YFF1002902), the National Natural Science Foundation of China (31730008, 32070199), and the Natural Science Foundation of Shandong Province (ZR2022JQ12).

AUTHOR CONTRIBUTIONS

Y.H.S. and X.S.Z. designed the research. Y.Y., H.Y., J.P., W.J.Y., F.L.Z., S.R.W., Y.Z., and X.Y.Z. performed the research. Y.Y. and Y.P.W. analyzed the data. Y.H.S. and X.S.Z. wrote the paper.

ACKNOWLEDGMENTS

We would like to thank Prof. Jiajie Wu and Prof. Fei Ni (College of Agronomy, Shandong Agricultural University) for providing the PBUE413, *Ubi*$_{pro}$*:GUS*, and PC186 vectors, as well as the Kronos and Langdon wheat seeds. We thank Prof. Dajian Zhang (College of Agronomy, Shandong Agricultural University) for providing Dongnong-50 soybean seeds. We also thank Prof. Jian Xu (Radboud Institute for Biological and Environmental Sciences, Radboud University) for providing the PBI106 vector. No conflict of interest is declared.

Received: July 16, 2023
Revised: October 12, 2023
Accepted: October 21, 2023
Published: October 28, 2023

REFERENCES

Altpeter, F., Springer, N.M., Bartley, L.E., Blechl, A.E., Brutnell, T.P., Citovsky, V., Conrad, L.J., Gelvin, S.B., Jackson, D.P., Kausch, A.P., et al. (2016). Advancing Crop Transformation in the Era of Genome Editing. Plant Cell **28**:1510–1520.

Bouchabke-Coussa, O., Obellianne, M., Linderme, D., Montes, E., Maia-Grondard, A., Vilaine, F., and Pannetier, C. (2013). Wuschel overexpression promotes somatic embryogenesis and induces organogenesis in cotton (Gossypium hirsutum L.) tissues cultured in vitro. Plant Cell Rep. **32**:675–686.

Boutilier, K., Offringa, R., Sharma, V.K., Kieft, H., Ouellet, T., Zhang, L., Hattori, J., Liu, C.M., van Lammeren, A.A.M., Miki, B.L.A., et al. (2002). Ectopic expression of BABY BOOM triggers a conversion from vegetative to embryonic growth. Plant Cell **14**:1737–1749.

Cheng, Z.J., Wang, L., Sun, W., Zhang, Y., Zhou, C., Su, Y.H., Li, W., Sun, T.T., Zhao, X.Y., Li, X.G., et al. (2013). Pattern of auxin and cytokinin responses for shoot meristem induction results from the regulation of cytokinin biosynthesis by AUXIN RESPONSE FACTOR3. Plant Physiol. **161**:240–251.

Chen, K., Wang, Y., Zhang, R., Zhang, H., and Gao, C. (2019). CRISPR/Cas Genome Editing and Precision Plant Breeding in Agriculture. Annu. Rev. Plant Biol. **70**:667–697.

Chen, Z., Debernardi, J.M., Dubcovsky, J., and Gallavotti, A. (2022). Recent advances in crop transformation technologies. Nat. Plants **8**:1343–1351.

Debernardi, J.M., Tricoli, D.M., Ercoli, M.F., Hayta, S., Ronald, P., Palatnik, J.F., and Dubcovsky, J. (2020). A GRF-GIF chimeric protein improves the regeneration efficiency of transgenic plants. Nat. Biotechnol. **38**:1274–1279.

Fehér, A. (2015). Somatic embryogenesis - Stress-induced remodeling of plant cell fate. Biochim. Biophys. Acta **1849**:385–402.

Florez, S.L., Erwin, R.L., Maximova, S.N., Guiltinan, M.J., and Curtis, W.R. (2015). Enhanced somatic embryogenesis in Theobroma cacao using the homologous BABY BOOM transcription factor. BMC Plant Biol. **15**:121.

Frame, B., Main, M., Schick, R., and Wang, K. (2011). Genetic transformation using maize immature zygotic embryos. Methods Mol. Biol. **710**:327–341.

Gallavotti, A., Zhao, Q., Kyozuka, J., Meeley, R.B., Ritter, M.K., Doebley, J.F., Pè, M.E., and Schmidt, R.J. (2004). The role of barren stalk1 in the architecture of maize. Nature **432**:630–635.

Gao, H., Gadlage, M.J., Lafitte, H.R., Lenderts, B., Yang, M., Schroder, M., Farrell, J., Snopek, K., Peterson, D., Feigenbutz, L., et al. (2020). Superior field performance of waxy corn engineered using CRISPR-Cas9. Nat. Biotechnol. **38**:579–581.

Gao, X., Chen, J., Dai, X., Zhang, D., and Zhao, Y. (2016). An Effective Strategy for Reliably Isolating Heritable and Cas9-Free Arabidopsis Mutants Generated by CRISPR/Cas9-Mediated Genome Editing. Plant Physiol. **171**:1794–1800.

Hao, Q., Wang, W., Han, X., Wu, J., Lyu, B., Chen, F., Caplan, A., Li, C., Wu, J., Wang, W., et al. (2018). Isochorismate-based salicylic acid biosynthesis confers basal resistance to Fusarium graminearum in barley. Mol. Plant Pathol. **19**:1995–2010.

He, G., Zhang, Y., Liu, P., Jing, Y., Zhang, L., Zhu, Y., Kong, X., Zhao, H., Zhou, Y., and Sun, J. (2021). The transcription factor TaLAX1 interacts with Q to antagonistically regulate grain threshability and spike morphogenesis in bread wheat. New Phytol. **230**:988–1002.

Hellens, R.P., Allan, A.C., Friel, E.N., Bolitho, K., Grafton, K., Templeton, M.D., Karunairetnam, S., Gleave, A.P., and Laing, W.A. (2005). Transient expression vectors for functional genomics, quantification of promoter activity and RNA silencing in plants. Plant Methods **1**:13.

Hiei, Y., Ishida, Y., and Komari, T. (2014). Progress of cereal transformation technology mediated by Agrobacterium tumefaciens. Front. Plant Sci. **5**:628.

Hoerster, G., Wang, N., Ryan, L., Wu, E., Anand, A., McBride, K., Lowe, K., Jones, T., and Gordon-Kamm, B. (2020). Use of non-integrating Zm-Wus2 vectors to enhance maize transformation. Vitro Cell Dev. Biol. Plant **56**:265–279.

Ikeuchi, M., Iwase, A., Rymen, B., Lambolez, A., Kojima, M., Takebayashi, Y., Heyman, J., Watanabe, S., Seo, M., De Veylder, L., et al. (2017). Wounding Triggers Callus Formation via Dynamic Hormonal and Transcriptional. Plant Physiol. **175**:1158–1174.

Ikeuchi, M., Ogawa, Y., Iwase, A., and Sugimoto, K. (2016). Plant regeneration: cellular origins and molecular mechanisms. Development **143**:1442–1451.

Ishida, Y., Tsunashima, M., Hiei, Y., and Komari, T. (2015). Wheat (Triticum aestivum L.) transformation using immature embryos. Methods Mol. Biol. **1223**:189–198.

Iwase, A., Harashima, H., Ikeuchi, M., Rymen, B., Ohnuma, M., Komaki, S., Morohashi, K., Kurata, T., Nakata, M., Ohme-Takagi, M., et al. (2017). WIND1 Promotes Shoot Regeneration through Transcriptional Activation of ENHANCER OF SHOOT REGENERATION1 in Arabidopsis. Plant Cell **29**:54–69.

Jia, Y., Yao, X., Zhao, M., Zhao, Q., Du, Y., Yu, C., and Xie, F. (2015). Comparison of Soybean Transformation Efficiency and Plant Factors Affecting Transformation during the Agrobacterium Infection Process. Int. J. Mol. Sci. **16**:18522–18543.

Komatsu, K., Maekawa, M., Ujiie, S., Satake, Y., Furutani, I., Okamoto, H., Shimamoto, K., and Kyozuka, J. (2003). LAX and SPA: major regulators of shoot branching in rice. Proc. Natl. Acad. Sci. USA **100**:11765–11770.

Li, H., Ye, K., Shi, Y., Cheng, J., Zhang, X., and Yang, S. (2017a). BZR1 Positively Regulates Freezing Tolerance via CBF-Dependent and CBF-Independent Pathways in Arabidopsis. Mol. Plant **10**:545–559.

Li, S., Cong, Y., Liu, Y., Wang, T., Shuai, Q., Chen, N., Gai, J., and Li, Y. (2017b). Optimization of Agrobacterium-Mediated Transformation in Soybean. Front. Plant Sci. **8**:246.

Li, Y.J., Yu, Y., Liu, X., Zhang, X.S., and Su, Y.H. (2021). The Arabidopsis MATERNAL EFFECT EMBRYO ARREST45 protein modulates

maternal auxin biosynthesis and controls seed size by inducing AINTEGUMENTA. Plant Cell **33**:1907–1926.

Liu, X., Bie, X.M., Lin, X., Li, M., Wang, H., Zhang, X., Yang, Y., Zhang, C., Zhang, X.S., and Xiao, J. (2023). Uncovering the transcriptional regulatory network involved in boosting wheat regeneration and transformation. Nat. Plants **9**:908–925.

Liu, Z., Wei, F., and Feng, Y.-Q. (2010). Determination of cytokinins in plant samples by polymer monolith microextraction coupled with hydrophilic interaction chromatography-tandem mass spectrometry. Anal. Methods **2**:1676–1685.

Lotan, T., Ohto, M., Yee, K.M., West, M.A., Lo, R., Kwong, R.W., Yamagishi, K., Fischer, R.L., Goldberg, R.B., and Harada, J.J. (1998). Arabidopsis LEAFY COTYLEDON1 is sufficient to induce embryo development in vegetative cells. Cell **93**:1195–1205.

Lowe, K., La Rota, M., Hoerster, G., Hastings, C., Wang, N., Chamberlin, M., Wu, E., Jones, T., and Gordon-Kamm, W. (2018). Rapid genotype "independent" Zea mays L. (maize) transformation via direct somatic embryogenesis. Vitro Cell Dev. Biol. Plant **54**:240–252.

Lowe, K., Wu, E., Wang, N., Hoerster, G., Hastings, C., Cho, M.J., Scelonge, C., Lenderts, B., Chamberlin, M., Cushatt, J., et al. (2016). Morphogenic Regulators Baby boom and Wuschel Improve Monocot Transformation. Plant Cell **28**:1998–2015.

Lu, H.P., Liu, S.M., Xu, S.L., Chen, W.Y., Zhou, X., Tan, Y.Y., Huang, J.Z., and Shu, Q.Y. (2017). CRISPR-S: an active interference element for a rapid and inexpensive selection of genome-edited, transgene-free rice plants. Plant Biotechnol. J. **15**:1371–1373.

McSteen, P., and Leyser, O. (2005). Shoot branching. Annu. Rev. Plant Biol. **56**:353–374.

Meng, W.J., Cheng, Z.J., Sang, Y.L., Zhang, M.M., Rong, X.F., Wang, Z.W., Tang, Y.Y., and Zhang, X.S. (2017). Type-B ARABIDOPSIS RESPONSE REGULATORs Specify the Shoot Stem Cell Niche by Dual Regulation of WUSCHEL. Plant Cell **29**:1357–1372.

Paek, K.Y., and Hahn, E.J. (2000). Cytokinins, auxins and activated charcoal affect organogenesis and anatomical characteristics of shoot-tip cultures of Lisianthus [Eustomagrandiflorum (Raf.) Shinn]. In Vitro Cell. Dev. Biol.-Plant **36**:128–132.

Qiu, F., Xing, S., Xue, C., Liu, J., Chen, K., Chai, T., and Gao, C. (2022). Transient expression of a TaGRF4-TaGIF1 complex stimulates wheat regeneration and improves genome editing. Sci. China Life Sci. **65**:731–738.

Ritter, M.K., Padilla, C.M., and Schmidt, R.J. (2002). The maize mutant barren stalk1 is defective in axillary meristem development. Am. J. Bot. **89**:203–210.

Schmitz, G., and Theres, K. (2005). Shoot and inflorescence branching. Curr. Opin. Plant Biol. **8**:506–511.

Shrawat, A.K., and Lörz, H. (2006). Agrobacterium-mediated transformation of cereals: a promising approach crossing barriers. Plant Biotechnol. J. **4**:575–603.

Skirpan, A., Wu, X., and McSteen, P. (2008). Genetic and physical interaction suggest that BARREN STALK 1 is a target of BARREN INFLORESCENCE2 in maize inflorescence development. Plant J. **55**:787–797.

Su, Y.H., Zhou, C., Li, Y.J., Yu, Y., Tang, L.P., Zhang, W.J., Yao, W.J., Huang, R., Laux, T., and Zhang, X.S. (2020). Integration of pluripotency pathways regulates stem cell maintenance in the Arabidopsis shoot meristem. Proc. Natl. Acad. Sci. USA **117**:22561–22571.

Tang, L.P., Zhang, X.S., and Su, Y.H. (2020). Regulation of cell reprogramming by auxin during somatic embryogenesis. aBIOTECH **1**:185–193.

Wang, K., Liu, H., Du, L., and Ye, X. (2017). Generation of marker-free transgenic hexaploid wheat via an Agrobacterium-mediated co-transformation strategy in commercial Chinese wheat varieties. Plant Biotechnol. J. **15**:614–623.

Wang, K., Shi, L., Liang, X., Zhao, P., Wang, W., Liu, J., Chang, Y., Hiei, Y., Yanagihara, C., Du, L., et al. (2022a). The gene TaWOX5 overcomes genotype dependency in wheat genetic transformation. Nat. Plants **8**:110–117.

Wang, Y., He, S., Long, Y., Zhang, X., Zhang, X., Hu, H., Li, Z., Hou, F., Ge, F., Gao, S., et al. (2022b). Genetic variations in ZmSAUR15 contribute to the formation of immature embryo-derived embryonic calluses in maize. Plant J. **109**:980–991.

Woods, D.P., Hope, C.L., and Malcomber, S.T. (2011). Phylogenomic analyses of the BARREN STALK1/LAX PANICLE1 (BA1/LAX1) genes and evidence for their roles during axillary meristem development. Mol. Biol. Evol. **28**:2147–2159.

Xing, H.L., Dong, L., Wang, Z.P., Zhang, H.Y., Han, C.Y., Liu, B., Wang, X.C., and Chen, Q.J. (2014). A CRISPR/Cas9 toolkit for multiplex genome editing in plants. BMC Plant Biol. **14**:327.

Yang, F., Wang, Q., Schmitz, G., Müller, D., and Theres, K. (2012). The bHLH protein ROX acts in concert with RAX1 and LAS to modulate axillary meristem formation in Arabidopsis. Plant J. **71**:61–70.

Yao, H., Skirpan, A., Wardell, B., Matthes, M.S., Best, N.B., McCubbin, T., Durbak, A., Smith, T., Malcomber, S., and McSteen, P. (2019). The barren stalk2 Gene Is Required for Axillary Meristem Development in Maize. Mol. Plant **12**:374–389.

Zhang, G., Zhao, F., Chen, L., Pan, Y., Sun, L., Bao, N., Zhang, T., Cui, C.X., Qiu, Z., Zhang, Y., et al. (2019). Jasmonate-mediated wound signalling promotes plant regeneration. Nat. Plants **5**:491–497.

Zhang, Z., Belcram, H., Gornicki, P., Charles, M., Just, J., Huneau, C., Magdelenat, G., Couloux, A., Samain, S., Gill, B.S., et al. (2011). Duplication and partitioning in evolution and function of homoeologous Q loci governing domestication characters in polyploid wheat. Proc. Natl. Acad. Sci. USA **108**:18737–18742.

Zuo, J., Niu, Q.W., Ikeda, Y., and Chua, N.H. (2002a). Marker-free transformation: increasing transformation frequency by the use of regeneration-promoting genes. Curr. Opin. Biotechnol. **13**:173–180.

Zuo, J., Niu, Q.W., Frugis, G., and Chua, N.H. (2002b). The WUSCHEL gene promotes vegetative-to-embryonic transition in Arabidopsis. Plant J. **30**:349–359.

Plant Communications, Volume *5*

Supplemental information

Enhancing wheat regeneration and genetic transformation through overexpression of *TaLAX1*

Yang Yu, Haixia Yu, Jing Peng, Wang Jinsong Yao, Yi Peng Wang, Feng Li Zhang, Shi Rong Wang, Yajie Zhao, Xiang Yu Zhao, Xian Sheng Zhang, and Ying Hua Su

Supplemental Figures and legends

Supplemental Figure 1

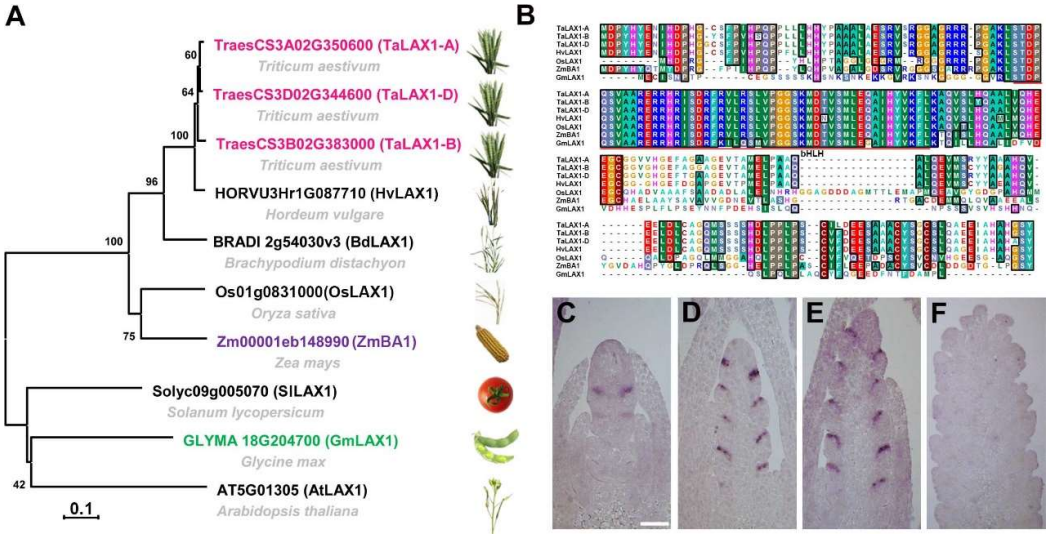

Supplemental Figure 1. Phylogenetic relationships among LAX1 homologous proteins and the expression pattern of *TaLAX1* in the development of wheat spikes. (Supports Figures 1 and 7)

(A) Phylogenetic trees of LAX1 homologous proteins for wheat (*Triticum aestivum*), barley (*Hordeum vulgare*), Brachypodium (*Brachypodium distachyon*), rice (*Oryza sativa*), maize (*Zea mays*), tomato (*Solanum lycopersicum*), soybean (*Glycine max*) and Arabidopsis (*Arabidopsis thaliana*). The evolutionary analysis was conducted based on OsLAX1 protein sequences in MEGA 11 using the neighbor-joining method.

(B) Comparison of the predicted amino acid sequences of TaLAX1-A/B/D, HvLAX1, OsLAX1, ZmBA1, and GmLAX1 proteins. The basic helix-loop-helix (bHLH) domain is indicated by a red horizontal line.

(C-F) RNA *in situ* hybridizations analyses indicate the expression pattern of *TaLAX1* at the single ridge stage **(C)**, double ridge stage **(D)**, glume primordium differentiation stage **(E)** and floret differentiation stage **(F)** of the Chinese Spring wheat spikes. An antisense probe derived from the whole coding region of *TaLAX1-A* was used. Scale bar = 200 μm.

Supplemental Figure 2

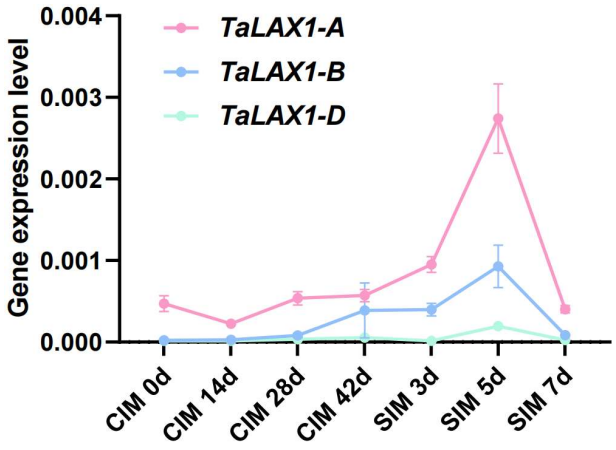

Supplemental Figure 2. Expression level of *TaLAX1-A*/*B*/*D* in the regeneration process of Chinese Spring. (Supports Figure 1)

Values are means ± SD, calculated from three individual experiments.

Supplemental Figure 3

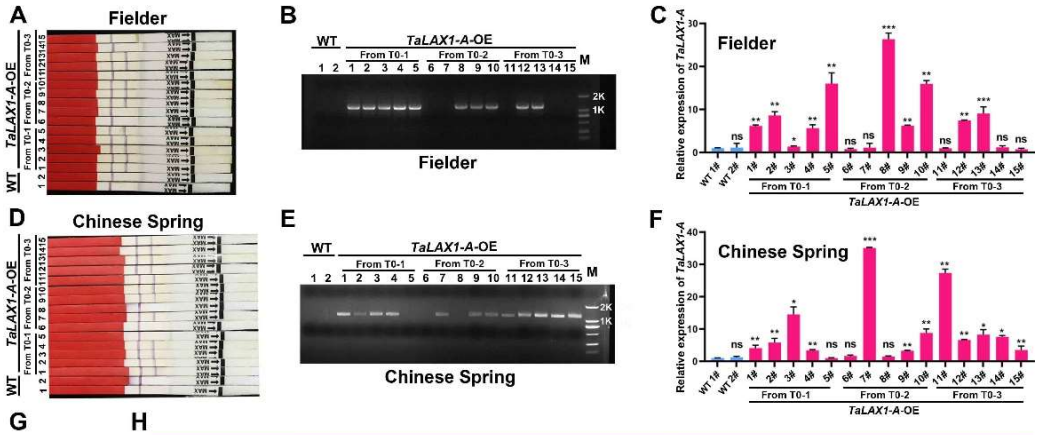

G

H

Fielder	Effective tiller number	Spike length (cm)	Grain number per spike	Thousand grain weight (g)	Grain yield per plant (g)	Plant height (cm)
Control	14.59±1.25	10.10±0.15	60.06±2.24	34.65±0.88	21.84±1.64	74.85±1.20
TaLAX1-A-OE	20.40±1.57	11.24±0.13	63.17±1.47	27.94±0.51	27.64±3.09	78.68±1.29
P-value	0.0064	<0.0001	0.2462	0.0009	0.0737	0.0436

I

J

Chinese Spring	Effective tiller number	Spike length (cm)	Grain number per spike	Thousand grain weight (g)	Grain yield per plant (g)	Plant height (cm)
Control	31.74±3.39	8.32±0.10	47.56±2.15	30.80±0.36	41.13±4.62	112.10±0.89
TaLAX1-A-OE	42.13±3.75	11.68±0.13	47.74±2.28	26.65±0.64	51.04±8.49	116.28±1.33
P-value	0.0476	<0.0001	0.9569	0.0026	0.2799	0.0200

Supplemental Figure 3. T1 progeny of *TaLAX1-A*-OE transgenic lines in Fielder and Chinese Spring. (Supports Figure 3)

(A-C) Identification of putative T1 progeny of *TaLAX1-A*-OE transgenic lines from 3 T0 lines in Fielder by QuickStix strips for the Bar protein **(A)**, amplification of transgenic-specific PCR product **(B)** and RT-qPCR analysis **(C)**. 2K: 2000 bp, 1K: 1000 bp, M: DNA marker.

(D-F) Identification of putative T1 progeny of *TaLAX1-A*-OE transgenic lines from 3 T0 lines in Chinese Spring by QuickStix strips for the Bar protein **(D)**, amplification of transgenic-specific PCR product **(E)** and RT-qPCR analysis **(F)**. 2K: 2000 bp, 1K: 1000 bp, M: DNA marker.

(G) Spike phenotypes the T1 progeny of non-transgenic lines (control) or *TaLAX1-A*-OE transgenic lines in Fielder. Scale bar = 1 cm.

(H) Main agronomic characters of the T1 progeny of control or *TaLAX1-A*-OE transgenic lines in Fielder.

(I) Spike phenotypes of the T1 progeny of control or *TaLAX1-A*-OE transgenic lines in Chinese Spring. Scale bar = 1 cm.

(J) Main agronomic characters of the T1 progeny of control or *TaLAX1-A*-OE transgenic lines in Chinese Spring.

Values in **(C**, **F)** are means ± SD, values in **(H**, **J)** are means ± SEM. All experiments

48 in **(C**, **F)** were performed at least three times. The data in **(H**, **J)** presents a count of the
49 main agronomic characteristics for 15 positive transgenic lines of the T1 generation in
50 Fielder and 16 positive transgenic lines of the T1 generation in Chinese Spring,
51 respectively. *** $P < 0.001$; ** $P < 0.01$; * $P < 0.05$; ns, not significant (Student's *t*-test,
52 two-tailed).

Supplemental Figure 4

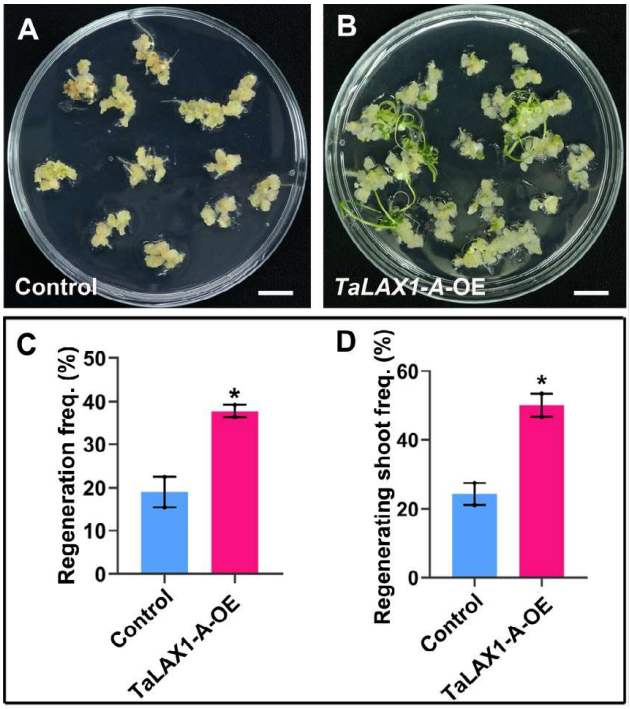

Supplemental Figure 4. Overexpression of *TaLAX1-A* promotes shoot regeneration after particle bombardment. (Supports Figures 1, 2 and 3)

(A) Shoot regeneration phenotypes of Fielder immature embryos infected with empty vector (control) by particle bombardment. Scale bar = 1 cm.

(B) Shoot regeneration phenotypes of Fielder immature embryos infected with *TaLAX1-A*-OE by particle bombardment. Scale bar = 1 cm.

(C) Regeneration frequencies of Fielder immature embryos infected with control or *TaLAX1-A*-OE vector by particle bombardment.

(D) Regenerating shoot frequencies of Fielder immature embryos infected with control or *TaLAX1-A*-OE vector by particle bombardment.

Values in **(C**, **D)** are means ± SEM from two independent experiments. Black points are the results from individual experiments. * $P < 0.05$ (Student's *t*-test, two-tailed).

Supplemental Figure 5

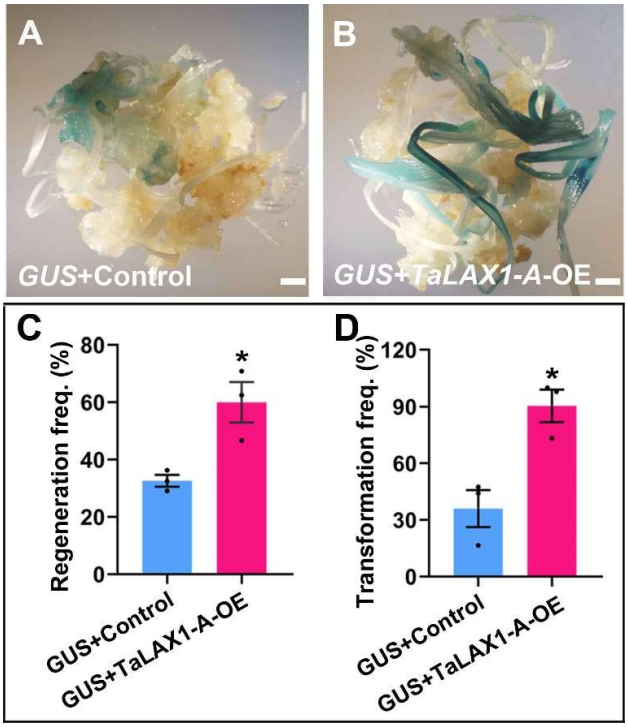

Supplemental Figure 5. Overexpression of *TaLAX1-A* promotes *GUS* transformation by two *Agrobacterium*-mediated co-transformation methods. (Supports Figure 4)

(A) and **(B)** show the shoot regeneration and transformation phenotypes of Fielder immature embryos infected with a mixture of *Agrobacterium* strains. *Agrobacterium* suspensions containing *GUS* and empty vector (control) were mixed together in a 1:1 ratio **(A)**, *GUS* and *TaLAX1-A*-OE were mixed together in a 1:1 ratio **(B)**. Scale bar = 2mm.

(C) Regeneration frequencies of Fielder immature embryos infected with mixtures of different Agrobacterium strains.

(D) Transformation frequencies of Fielder immature embryos infected with mixtures of different Agrobacterium strains.

Values in **(C**, **D)** are means ± SEM from three independent experiments. Black points are the results from individual experiments. * $P < 0.05$ (Student's *t*-test, two-tailed).

Supplemental Figure 6

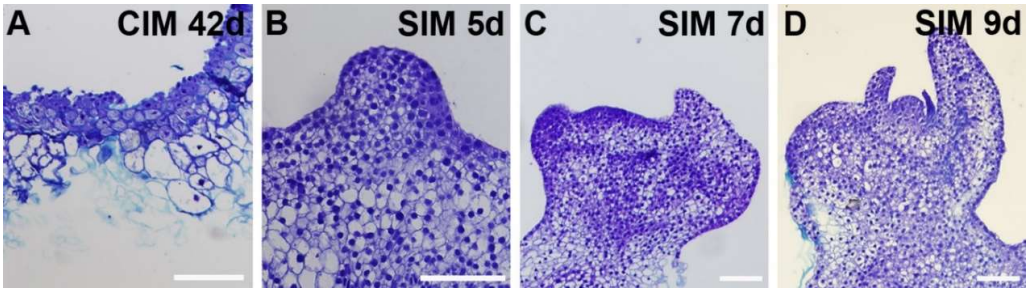

Supplemental Figure 6. Paraffin sections of the shoot regeneration process of Chinese Spring. (Supports Figure 5)

(A) The immature embryos of Chinese Spring were cultured on CIM for 42 days. Scale bar = 200 µm.

(B-D) The immature embryos of Chinese Spring were cultured on CIM for 42 days, followed by incubation on SIM for 5 days **(B)**, 7 days **(C)** or 9 days **(D)**. Scale bar = 200 µm.

Supplemental Figure 7

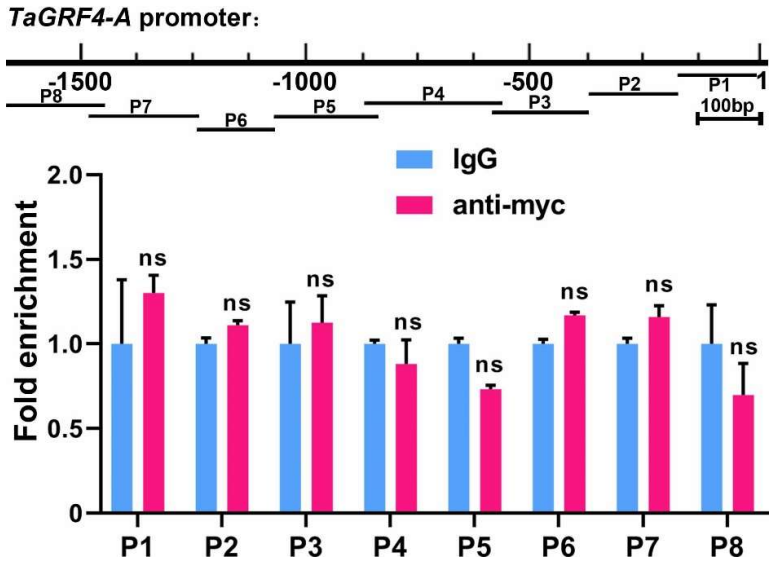

Supplemental Figure 7. TaLAX1-A does not bind to the *TaGRF4-A* promoter. (Supports Figure 5)

ChIP-qPCR of the *TaGRF4-A* promoter using an anti-*myc* antibody in the *TaLAX1-A*-OE transgenic plants, negative controls used IgG antibody on *TaLAX1-A*-OE samples. There was no enrichment of fragments. Values are means ± SD from three independent experiments. ns, not significant (Student's *t*-test, two-tailed).

Supplemental Figure 8

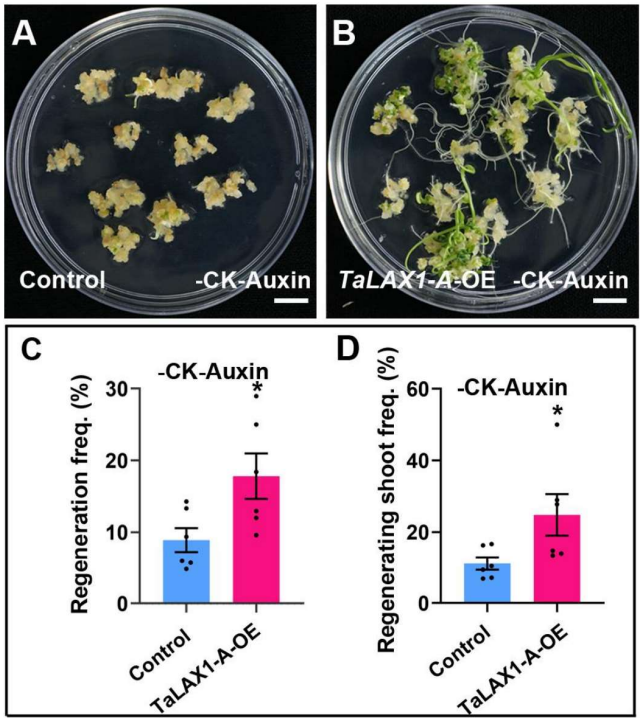

Supplemental Figure 8. Effect of *TaLAX1-A* overexpression on shoot regeneration in the absence of exogenous cytokinin and auxin. (Supports Figure 6)

(A) Shoot regeneration phenotypes of Fielder immature embryos cultured on CIM (without exogenous auxin) for 42 days and on SIM (without exogenous cytokinin) for 20 days after infection with empty vector (control). Scale bar = 1 cm.

(B) Shoot regeneration phenotypes of Fielder immature embryos cultured on CIM (without exogenous auxin) for 42 days and on SIM (without exogenous cytokinin) for 20 days after infection to introduce the *TaLAX1-A*-OE vector. Scale bar = 1 cm.

(C) Regeneration frequencies of Fielder immature embryos cultured on CIM (without exogenous auxin) for 42 days and on SIM (without exogenous cytokinin) for 20 days after infection to introduce the control or *TaLAX1-A*-OE vector.

(D) Regenerating shoot frequencies of Fielder immature embryos cultured on CIM (without exogenous auxin) for 42 days and on SIM (without exogenous cytokinin) for 20 days after infection to introduce the control or *TaLAX1-A*-OE vector.

Values in **(C**, **D)** are means ± SEM from six independent experiments. Black points indicate results from individual experiments. * $P < 0.05$ (Student's *t*-test, two-tailed).

Supplemental Figure 9

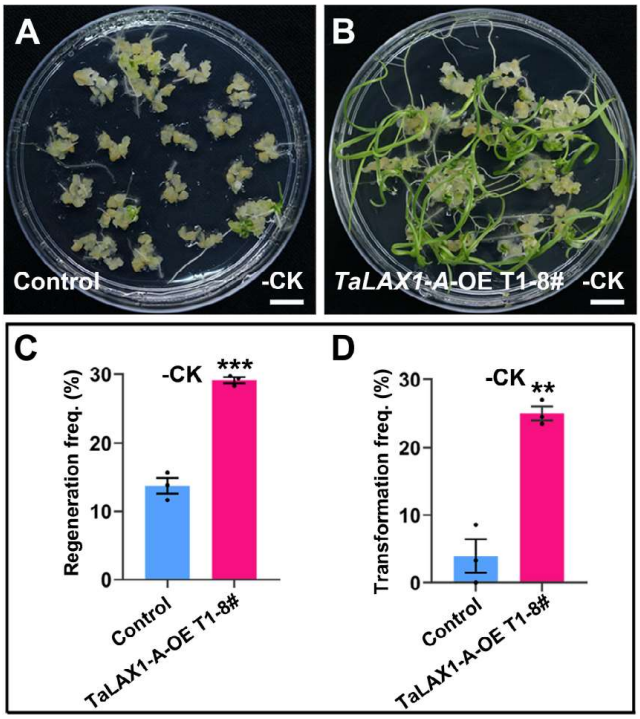

Supplemental Figure 9. Regeneration and transformation of T1 progeny of *TaLAX1-A*-OE transgenic lines in the absence of exogenous cytokinin. (Supports Figure 6)

(A) Fielder immature embryos from T1 progeny of non-transgenic lines (control) were cultured on CIM for 42 days and on SIM (without exogenous cytokinin) for 20 days after infection with the Ubi_{pro}*:GUS* vector. Scale bar = 1 cm.

(B) Fielder immature embryos from T1 progeny of *TaLAX1-A*-OE lines were cultured on CIM for 42 days and on SIM (without exogenous cytokinin) for 20 days after infection with the Ubi_{pro}*:GUS* vector. Scale bar = 1 cm.

(C) Regeneration frequencies of immature embryos of control or *TaLAX1-A*-OE transgenic lines infected with the Ubi_{pro}*:GUS* vector in the absence of cytokinin.

(D) Transformation frequencies of immature embryos of control or *TaLAX1-A*-OE transgenic lines infected with the Ubi_{pro}*:GUS* vector in the absence of cytokinin.

Values in **(C**, **D)** are means ± SEM from three independent experiments. Black points are the results from individual experiments. *** $P < 0.001$; ** $P < 0.01$ (Student's *t*-test, two-tailed).

Supplemental Figure 10

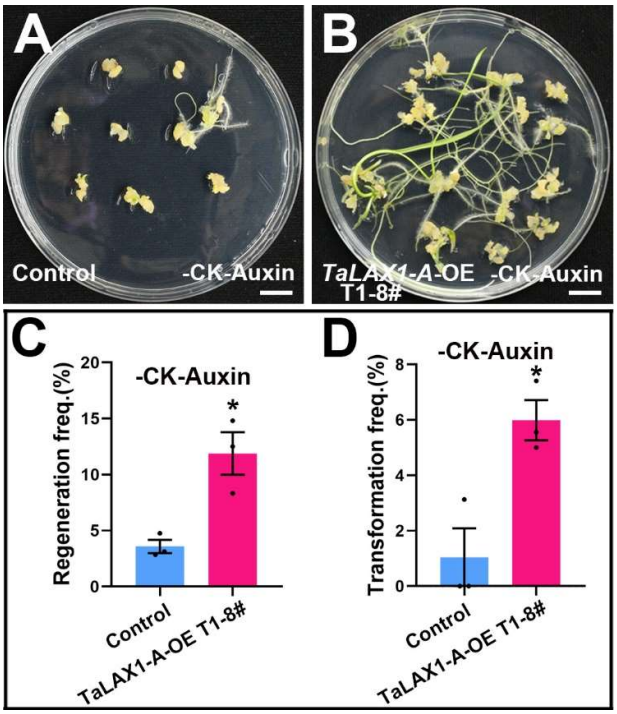

Supplemental Figure 10. Regeneration and transformation of T1 progeny of *TaLAX1-A*-OE transgenic lines in the absence of exogenous cytokinin and auxin. (Supports Figure 6)

(A) Fielder immature embryos from T1 progeny of non-transgenic lines (control) were cultured on CIM (without exogenous auxin) for 42 days and on SIM (without exogenous cytokinin) for 20 days after infection with the *Ubi$_{pro}$:GUS* vector. Scale bar = 1 cm.

(B) Fielder immature embryos from T1 progeny of *TaLAX1-A*-OE lines were cultured on CIM (without exogenous auxin) for 42 days and on SIM (without exogenous cytokinin) for 20 days after infection with the *Ubi$_{pro}$:GUS* vector. Scale bar = 1 cm.

(C) Regeneration frequencies of immature embryos of control or *TaLAX1-A*-OE transgenic lines infected with the *Ubi$_{pro}$:GUS* vector in the absence of cytokinin and auxin.

(D) Transformation frequencies of immature embryos of control or *TaLAX1-A*-OE transgenic lines infected with the *Ubi$_{pro}$:GUS* vector in the absence of cytokinin and auxin .

Values in **(C**, **D)** are means ± SEM from three independent experiments. Black points are the results from individual experiments. * $P < 0.05$ (Student's *t*-test, two-tailed).

Supplemental Figure 11

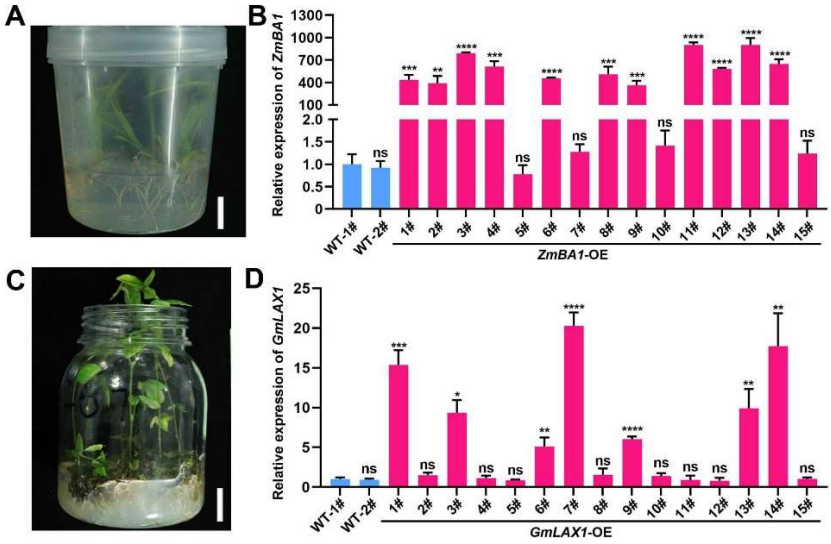

Supplemental Figure 11. Identification of putative T0 progeny of *ZmBA1*-OE or *GmLAX1*-OE transgenic lines. (Supports Figure 7)

(A) Plants obtained from regenerated shoots induced by *ZmBA1*-OE on a rooting medium for root elongation. Scale bar = 1 cm.

(B) Identification of putative T0 progeny of *ZmBA1*-OE transgenic lines by RT-qPCR analysis.

(C) Plants obtained from regenerated shoots induced by *GmLAX1*-OE on a rooting medium for root elongation. Scale bar = 2 cm.

(D) Identification of putative T0 progeny of *GmLAX1*-OE transgenic lines by RT-qPCR analysis.

Values in **(B, D)** are means ± SD, all experiments were performed at least three times. **** $P < 0.0001$; *** $P < 0.001$; ** $P < 0.01$; * $P < 0.05$; ns, not significant (Student's *t*-test, two-tailed).